Tracing the North Atlantic Deep Water through the Romanche and Chain fracture zones with chlorofluoromethanes

M.-J. Messias[a,b], C. Andrié[a], L. Mémery[a,*], H. Mercier[c]

[a]*Laboratoire d'Océanographie Dynamique et de Climatologie (CNRS/ORSTOM/UPMC),*
Institut Pierre Simon Laplace, Université Pierre et Marie Curie, 4 place Jussieu, 75005 PARIS, France
[b]*Laboratoire de Modélisation Climatique et de l'Environement (LMCE), CEN SACLAY,*
91119 GIF SUR YVETTE, France
[c]*Laboratoire de Physique des Océans, (CNRS/IFREMER/UBO), IFREMER centre de Brest,*
BP 70 29280 PLOUZANE, France

Abstract

Chlorofluoromethanes (CFMs) F-11 and F-12 were measured during August 1991 and November 1992 in the Romanche and Chain Fracture Zones in the equatorial Atlantic. The CFM distributions showed the two familiar signatures of the more recently ventilated North Atlantic Deep Water (NADW) seen in the Deep Western Boundary Current (DWBC). The upper maximum is centered around 1600 m at the level of the Upper North Atlantic Deep water (UNADW) and the deeper maximum around 3800 m at level of the Lower North Atlantic Deep Water (LNADW). These observations suggest a bifurcation at the western boundary, some of the NADW spreading eastward with the LNADW entering the Romanche and the Chain Fracture Zones. The upper core ($\sigma_{1.5} = 34.70$ kg m^{-3}) was observed eastward as far as 5°W. The deep CFM maximum ($\sigma_4 = 45.87$ kg m^{-3}), associated with an oxygen maximum, decreased dramatically at the sills of the Romanche Fracture Zone: east of the sills, the shape of the CFM profiles reflects mixing and deepening of isopycnals. Mean apparent water "ages" computed from the F-11/F-12 ratio are estimated. Near the bottom, no enrichment in CFMs is detected at the entrance of the fracture zones in the cold water mass originating from the Antarctic Bottom Water flow. © 1999 Elsevier Science Ltd. All rights reserved.

*Corresponding author. Fax: 00331 44 277159; e-mail: memery@lodyc.jussieu.fr

1. Introduction

Deep waters (colder than 4°C potential temperature) represent the major part of the world ocean water masses. Formed at high latitudes, the cold and dense North Atlantic Deep Water (NADW) and Antarctic Bottom Water (AABW) flow through the Atlantic Ocean as deep western boundary currents. The deep Atlantic ocean is divided into two basins, west and east by the Mid-Atlantic Ridge (MAR). The contribution of the MAR fracture zones, which allow the passage of the deep and bottom waters from the western to the eastern basins, is a key issue in understanding the ventilation and circulation of the deep ocean (Mantyla and Reid, 1983). Evidence of the impact of the fracture zones on the circulation between the two basins has been shown in the Charlie-Gibbs Fracture Zone (westward flux of overflow ~ 2.4 Sv: 1 Sv $= 1 \times 10^6 \, m^3 \, s^{-1}$) near 53°N (Saunders, 1994) and in the Vema Fracture Zone at mid-latitude around 11°N (geostrophic transport colder than 2.0°C ~ 2 Sv at the Vema exit, McCartney et al., 1991). The present paper focuses on the Romanche and the Chain Fracture Zones (referred to as RFZ and CFZ in the following), which are both possible pathways for the LNADW (Lower North Atlantic Deep Water) and the AABW across the MAR at the equator (Fig. 1). Some authors (Speer and McCartney, 1991; Friedrichs and Hall, 1993) have examined the splitting of the Deep Western Boundary Current (DWBC) eastward near the equator and confirmed the role of these equatorial fracture zones in guiding the circulation of deep water. Mercier et al. (1994) have described the pathways followed by the AABW through the equatorial fracture zones. The transport of bottom water through these fracture zones has been indirectly estimated to be comprised between 2.6 to 5.1 Sv for water colder than 2.07°C by Schlitzer (1987), and to be ~ 2 Sv for water below 4000 m depth by Warren and Speer (1991). Recent direct velocity measurements (Mercier and Speer, 1998) estimated an eastward bottom water transport of 1.2 Sv.

Based on the hydrographic background of the region and previous tracer studies (Metclaf et al., 1964; Heezen et al., 1964; Weiss et al., 1985; Schlitzer, 1987), we expected to find recently ventilated deep water with detectable anthropogenic chlorofluoromethanes (CFMs or freons) in these passages. Released to the atmosphere since the early 1930s, CFMs have tagged the surface ocean and entered the ocean interior in the areas of deep water formation, providing a very useful tool for the investigation of the circulation of newly formed water masses (Bullister, 1989). Ten years ago, during the Transient Tracers in the Ocean (TTO) program, the Upper North Atlantic Deep Water (UNADW) was traced using its core property of CFM maximum from the Labrador Sea along the western boundary (Weiss et al., 1985). The signal has reached the equator, where it is found in the DWBC at a depth of about 1600 m (density anomaly relative to 1500 m, $\sigma_{1.5} = 34.63 \, kg \, m^{-3}$). There, this water mass bifurcates, part extending east along the equator and part continuing south in the Brazil Basin DWBC. Fine and Molinari (1988), Molinari et al. (1992), and Rhein et al. (1995) have observed two cores of high CFMs in the DWBC between 26.5°N and 13°N, 14.5°N and the equator, and downstream of 5°S, respectively: the shallow UNADW core mentioned previously and a deeper core at about 3000–4000 m corresponding to the LNADW. Along the equator, CFM concentrations have also been measured near
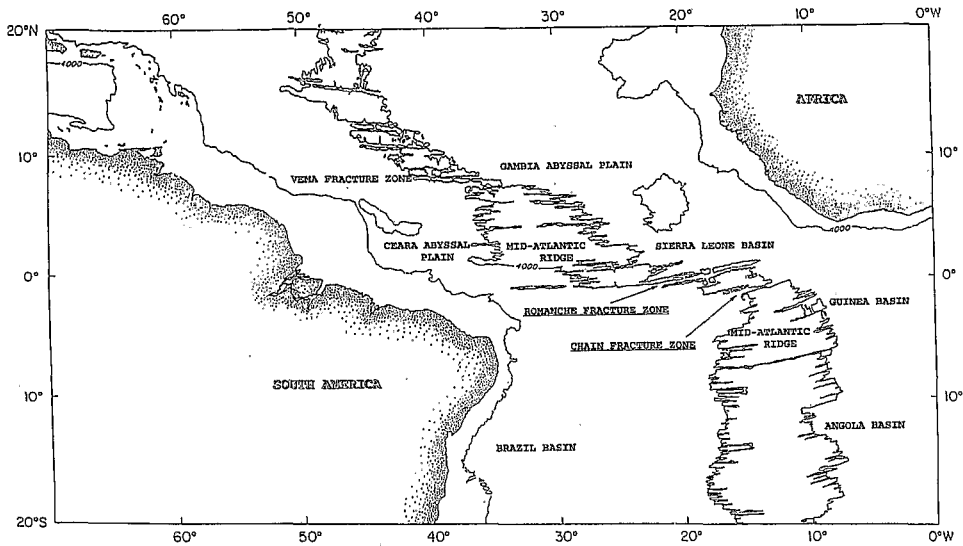
Fig. 1. Bathymetry of the Equatorial Atlantic showing the location of the Romanche and Chain Fracture Zones in the Mid-Atlantic-Ridge. Adapted from GEBCO (1978).

1400–2250 and 4000 dbar (Doney and Bullister, 1992; Andrié et al., 1998). Using CFM concentrations, the northward spreading of AABW has been observed as far as 5°S in the Brazil basin (Andrié et al., 1998; Rhein et al., 1995).

The present paper is structured as follows. Section 2 is a presentation of both the Romanche cruises and the experimental methods. In Section 3, we describe and analyze the characteristics of the deep and bottom water masses at the entrance of the RFZ and CFZ as well as the CFM spatial distributions along these fracture zones. In Section 4 and 5, we describe the CFM maxima and the transformations of the water masses as they flow eastwards. In Section 6, we then compute the CFM ratio and estimate the "apparent ages" of the deep water masses tagged by the CFM extrema as well as the "apparent dilution" factors. Finally, Section 7 gives a summary and some concluding remarks.

2. Data

The Romanche 1 and 2 cruises were part of the Deep Basin Experiment (DBE) of the World Ocean Circulation Experiment (WOCE). They consisted of bathymetric and hydrographic surveys of the Romanche and the Chain Fracture Zones (0°45′S and 19°W, 2°2′S and 15°W, respectively) from the *N.O. L'Atalante*. Maps of the area with the CFM station positions are shown in Fig. 2. Romanche 1 (August 10 to September 8, 1991) was an exploration of the hydrography and the bathymetry of the two fracture zones. A description of the bathymetry of the Romanche and Chain
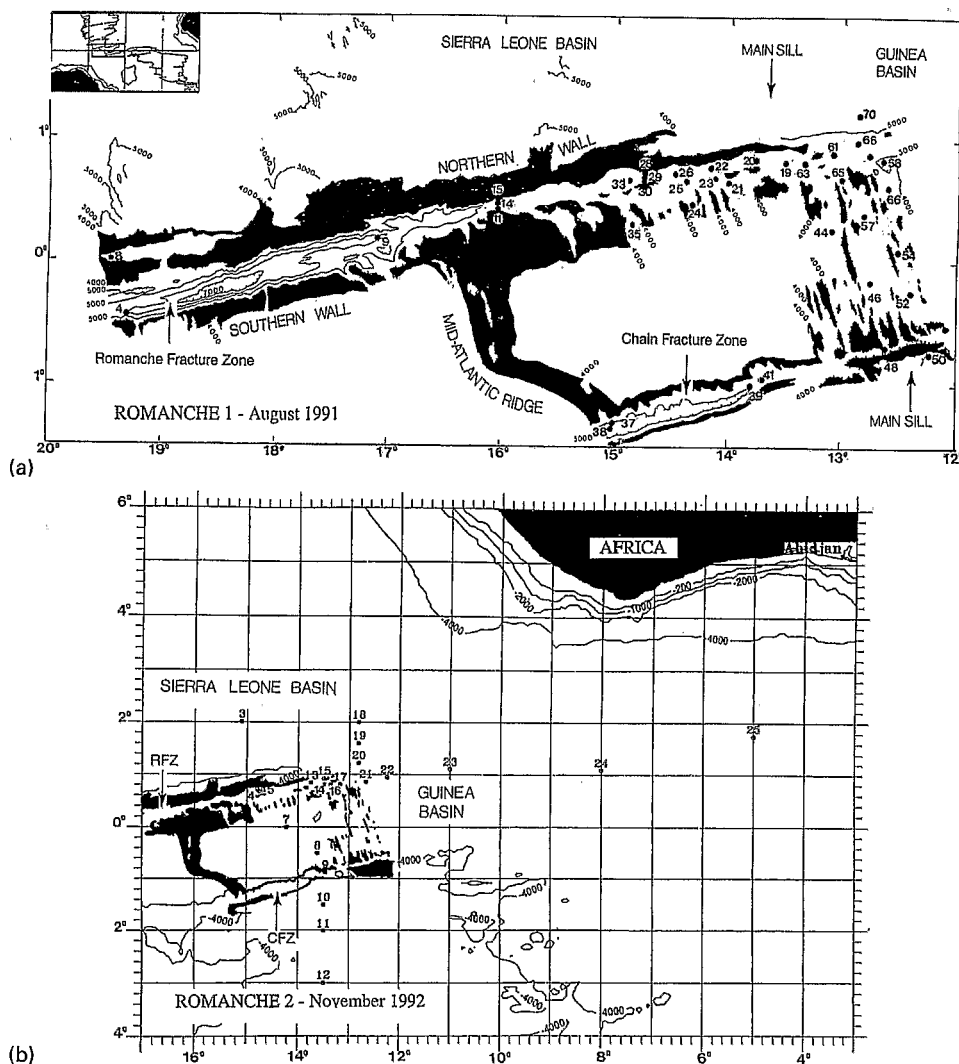
Fig. 2. Bathymetry of the Romanche and Chain Fracture Zones and CFM station locations (dots) occupied during (a) the Romanche 1 cruise and (b) the Romanche 2 cruise. Black areas indicate bottom depths less than 4000 m.

Fracture Zones has been published by Mercier et al. (1994). We summarize briefly the main structure of the bathymetry: the RFZ (about 800 km long) and CFZ (about 300 km long) are deep openings across the MAR that have average heights of about 3000 m (with summits from 3400 m to less than 2000 m). The width of the CFZ is narrower than that of the RFZ (5–20 km versus 10–40 km). The RFZ and CFZ main sills are found at depths of 4350 and 4050 m, respectively. In the eastern part of the

MAR, an alternating pattern of rises and valleys, referred to as the communication region by Mercier et al. (1994), connects the CFZ to the RFZ. During the Romanche 2 cruise (November 11 to 30, 1992), the hydrographic coverage was better resolved in the sill region and extended eastward.

At each station, 16–32 samples were taken from an 8 l sampling-bottle rosette equipped with a Neil Brown conductivity-temperature-depth-oxygen profiler (CTDO$_2$). The tabulated data, the calibration of the CTDO$_2$ measurements and the validation of the bottle data are published in data reports (Mercier et al., 1992; 1995). The error in the pressure was estimated to be ± 3 dbar. The errors in the oxygen, salinity and temperature are, respectively, on the order of ± 0.003 ml/l, ± 0.003 and $\pm 0.003°$C and those for nutrients (measured only during the cruise Romanche I with an Auto-Analyser II Technicon) of $\pm 0.1\%$.

The chlorofluoromethanes F-11 (CCl$_3$F) and F-12 (CCl$_2$F$_2$) were measured by electron capture detection gas chromatography coupled to a purge-and-trap extraction technique similar to that of Bullister and Weiss (1988). Samples were taken in glass syringes. On the Romanche 1 cruise, contamination problems precluded the use of the F-12 data for stations 4 to 39. The F-11 and F-12 data are reported on the SIO 1986 calibration scale. The atmospheric concentrations were estimated, with a precision of $\pm 1\%$ from daily measurements, to be 500.5 ppt (part per trillion) for F-12 and 268.4 ppt for F-11 during Romanche 1 and 515.5 ppt of F-12 and 275.3 ppt for F-11 during Romanche 2. The near surface equatorial Atlantic is subject to an intense seasonal upwelling that brings the water originally downwelled in the subtropical gyres to the surface, and we found a CFM saturation in surface water of about 88% during Romanche 1 (upwelling intensified in August) and 92% during Romanche 2 (November). All the CFM measurements were corrected for the sample blank (bottle, glass syringes, storage) and the analytical system blank. The blanks have been estimated from the CFM concentrations measured in assumed CFM-free deep water masses (i.e. Circumpolar Deep Waters). Because we observed an evolution of the blank values during the cruises, the blanks were estimated at each station. During Romanche 1, blanks for F-11 ranged from 0.008 to 0.021 pmol kg^{-1} (mean: 0.015 ± 0.004 pmol kg^{-1}). Blanks for F-12 ranged from 0.011 to 0.019 pmol kg^{-1} for station 41 to 71 (mean: 0.015 ± 0.003 pmol kg^{-1}). During the Romanche 2 cruise, blanks for F-11 were similar, with values from 0.008 to 0.019 (mean: 0.014 ± 0.004). For F-12, the blanks had lower values, from 0.005 to 0.013 (mean: 0.009 ± 0.003). In order to check the blank level of all hydrographic bottles, the entire rosette was tripped at a single depth (3000 dbar) in CFC-free water for the Romanche 2 cruise. The averages of the measurements (around 0.010 ± 0.005 pmol kg^{-1} for F-11 and 0.007 ± 0.003 pmol kg^{-1} for F-12 at the end of the cruise) on these samples were close to the blanks estimated by station. The standard deviation of the blanks (including the accuracy of the analytical system as well as the effects of contamination) determines the detection limit, which is around 0.005 pmol kg^{-1} for F-11 and 0.003 pmol kg^{-1} for F-12 for both cruises. Samples from deep levels were sometimes quite close to the detection limit, but the significant number of similarly measured values shows that they represent a real signal.

3. Observations

3.1. Water mass properties and CFM vertical profiles

The sources and the deep water mass characteristics in the equatorial Atlantic have been recently investigated by several authors (Weiss et al., 1985; Fine and Molinari, 1988; Pickart et al., 1989; Speer and McCartney, 1991; Molinari et al., 1992; Friedrichs and Hall, 1993; Smethie Jr., 1993; Rhein et al., 1995; Andrié et al., 1998). In particular, hydrography of the LNADW and the AABW along the RFZ and the CFZ during the cruise Romanche 1 has been presented by Mercier and Morin (1997). At the fracture entrances, the CFM distribution (Fig. 3) was found to be structured as in the DWBC (Fine and Molinari, 1988; Molinari et al., 1992). In the NADW, two familiar CFM maxima observed at 1600 and 3800 m appear as evidence of eastward feeding from the DWBC towards the fracture entrances of the recently ventilated components of the warm, saline, oxygen rich NADW. The fresh, low oxygen and high nutrient water masses of circumpolar origin (Reid, 1989) are found at 1000 and 3000 m depth and at the bottom below 4000 m, sandwiching the NADW. Circumpolar Deep Water (CDW) results from the mixing of deep-waters from the Indian, Pacific and Atlantic Oceans along a path around Antarctica. Due to the relatively long time since these deep waters were in contact with the atmosphere, these waters are CFM-free at the entrance to the RFZ and CFZ. Below we detail the main hydrographic characteristics of the deep-water masses in accordance with the CFM signals (Figs. 3 and 4).

The F-11 distribution clearly identifies the main components of the NADW. The upper F-11 maximum (>0.04 pmol kg^{-1}) coincides with the salinity maximum (34.98 at $\sigma_{1.5} = 34.66$ kg m^{-3}) of the UNADW that Wüst (1935) attributed to the Mediterranean Sea Water influence. It enhances the core of the most recently ventilated NADW originating from the southern Labrador Sea (Pickart, 1992). The F-11 core extends from 1300 to 1900 m depths and is centered around 1600–1700 m ($\sigma_{1.5} = 34.63$ kg m^{-3} and $\theta = 3.8°$C, all temperatures referred to in the following are potential temperatures). Between 1700 and 1800 m, it is associated with phosphate (1.1 μmol kg^{-1} at $\sigma_2 = 36.94$ kg m^{-3}) and silicate (20 μmol kg^{-1} at $\sigma_2 = 36.89$ kg m^{-3}) minima, as previously observed in the equatorial Atlantic (Weiss et al., 1985; Reid, 1989; Doney and Bullister, 1992). The top of the UNADW is marked here by a slight maximum in temperature of 4.42°C around 1200 m (1150–1300 m, $\sigma_0 = 27.6$ kg m^{-3}). Above, the first free-CFM level corresponds to the upper part of the Circumpolar Deep Water (UCDW), centered around 1000 m ($\sigma_0 = 27.3$ kg m^{-3}), in agreement with Reid's (1989) description of CDW at the equator. The UCDW is characterized by a minimum in temperature around 4.36°C and low oxygen values (162 μmol kg^{-1}). Here, it lies below the Antarctic Intermediate Water (AAIW), which is recognized by its salinity minimum (34.5) and silicate maximum (33.8 μmol kg^{-1}) at approximately 700–800 m. In the North Atlantic (Smethie, 1993) and downstream at 8°N (Molinari et al., 1992), the upper CFM core has been observed centered at 4.5°C. This suggests that the CFM maximum is truncated in the upper part of the UNADW by the UCDW at the equator as suggested by Rhein et al. (1995). The oxygen maximum
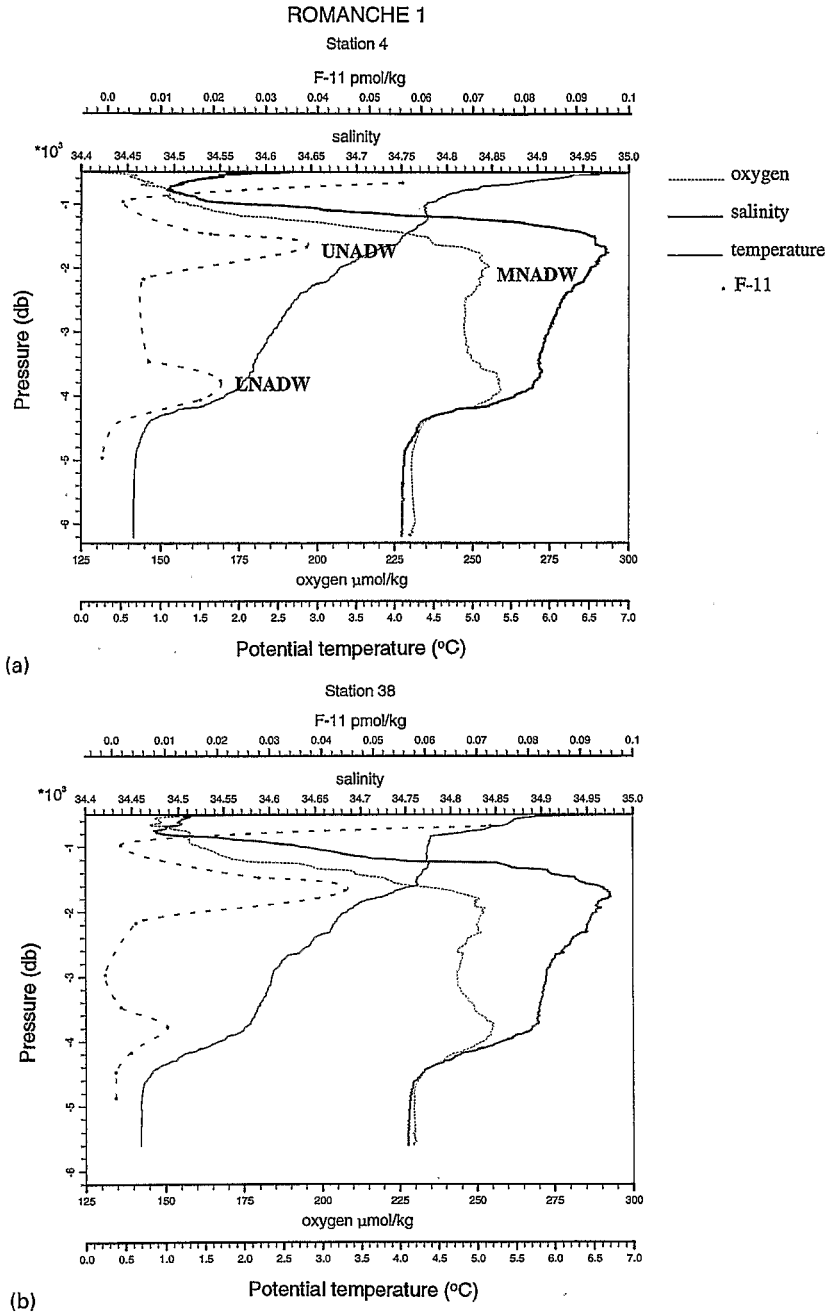
ROMANCHE 1

Station 4

(a)

Station 38

(b)

Fig. 3. Vertical profiles below 500 dbar of salinity, oxygen (μmol kg^{-1}), potential temperature (°C) from CTDO$_2$ data and F-11 (pmol kg^{-1}) from bottle samples (stars), for August 1991 (Romanche 1) from (a) station 4 (0°27S–19°18W) located at the entrance of the RFZ and (b) station 38 (1°22S–14°59W) located at the entrance of the CFZ. In (a) the core layers of several water masses referred to in the text are identified. UNADW, MNADW and LNADW are Upper, Middle, and Lower North Atlantic Deep Water, according to classification Wüst (1935).
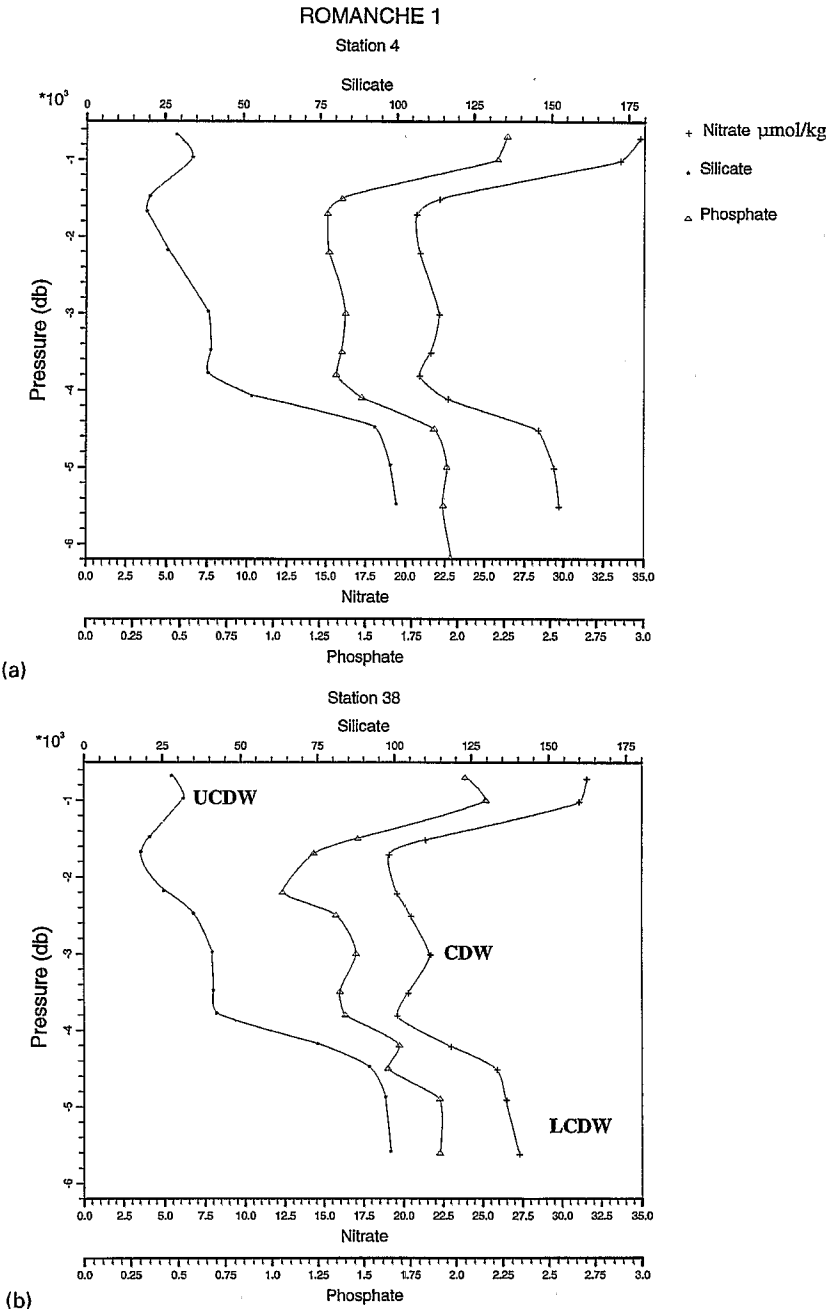
ROMANCHE 1

Station 4

(a)

Station 38

(b)

Fig. 4. Vertical profiles below 500 dbar of nitrate (μmol kg^{-1}), silicate (μmol kg^{-1}) and phosphate (μmol kg^{-1}) for August 1991 (Romanche 1) from (a) station 4 located at the entrance of the RFZ and (b) station 38 located at the entrance of the CFZ. In (b) the core layers of Circumpolar Deep Water (CDW) masses referred to in the text are identified. UCPW and LCDW are Upper and Lower Circumpolar Deep Water.

between 1700 and 2400 m depths defines the Middle North Atlantic Deep Water (MNADW) according to Wüst (1935). It is centered at about 2000 m ($\sigma_{1.5}$ = 34.7 kg m^{-3}, σ_2 = 36.95 kg m^{-3}) and is not associated with the CFM core. This oxygen maximum is thought to be the classical Labrador Sea Water (LSW; Pickart, 1992), which has been associated with a relative minimum of F-11 in the DWBC (Molinari et al., 1992). The upper part of the oxygen maximum overlaps the high salinity layer and the CFM signal, which decreases to undetectable levels around 2500 m. Below, the second CFM-free level (σ_4 = 45.83 kg m^{-3}) is associated with a minimum in oxygen and includes components of both NADW and CDW. The CFM free NADW component (2500–2900 m) corresponds to Gibbs Fracture Zone Water (GFZW), which is a mixture of Iceland Scotland Overflow Water (ISOW) and North East Atlantic water (NEAW) (Smethie, 1993; Reid, 1994; Rhein et al., 1995). The ISOW is fed by Norwegian Deep Water not recently renewed. Hence, the GFZW contributes little to the CFM signal when it joins the DWBC in the western Atlantic through the Gibbs Fracture Zone (Smethie, 1993). Moreover, Molinari et al. (1992), Rhein et al. (1995) and Andrié et al. (1998) suggest weak ventilation of the GFZW in the DWBC, which accentuates the CFM minimum. The Circumpolar Deep Water found beneath also has oxygen and CFM minima, but it is marked by a slight maximum in nitrate (1.39 μmol/l), phosphate (1.39 μmol/l) and silicate (39.8 μmol/l). In the DWBC, Molinari et al. (1992) attribute lower salinity near 3500 m to a water mass of circumpolar origin. The characteristics of this southern water mass are more marked in the range of 3000–3500 m (Fig. 4) at the CFZ (1.22°S) than at the RFZ (0.27°S) entrance and then decrease north-eastwards. The lower F-11 core, centered at 3800 m (σ_4 = 45.87 kg m^{-3}) tags the highly oxygenated (259 μmol kg^{-1}) and salty densest layer of the NADW (LNADW according to Wüst, 1935) originating from the Denmark Strait Overflow (DSOW). This F-11 maximum is lower (0.02 pmol kg^{-1}) than the maximum observed in the UNADW. The feeding of the DSOW used to be attributed principally to the upper Arctic Intermediate Water (Swift et al., 1980, Smethie, 1993) formed in the Iceland and Greenland Seas by winter convection. This water mass would exit the Nordic Seas through the Denmark Strait 1–2 years after its formation, loaded with high CFM concentrations (Smethie and Swift, 1989; Smethie, 1993). Recently, based on new data sets, on tracer conservation and considerations on heat fluxes, Mauritzen (1996) has presented an alternative to this classical scheme. After strong buoyancy losses during their northward journey in the Norwegian sea, Atlantic waters are carried into the Arctic Ocean. They are then modified and flow back southward through the Fram Strait, in the East Greenland Current, with considerable speed, and almost no mixing. The LNADW at the entrance of the fracture zones is associated with minima in silicate and phosphate. The temperature range of the lower F-11 core was found between 2.2°C and around 1.6–1.5°C. The historic delineation for AABW, 1.9°C (McCartney and Curry, 1993), corresponds in our data to the lower CFM maximum, certainly due to upstream vertical mixing between the AABW and the LNADW (Mercier and Morin, 1997). The transition between the LNADW and AABW corresponds to important monotonic gradients. Below 4700 m, the profiles are homogeneous in temperature (0.75–0.62°C), salinity (34.76–34.75), oxygen (231.6–230.4 μmol kg^{-1}) and density (45.997 < σ_4 < 46.001).

These characteristics associated with a CFM free level, a silicate (100 µmol kg^{-1}) and a phosphate maximum (1.96 µmol kg^{-1}) identify the Lower Circumpolar Deep Water (LCDW with $\sigma_4 > 45.92$), which is less dense than the other component of AABW, i.e. the oxygen-CFM-rich Weddell Sea Deep Water ($46.006 < \sigma_4$). The Weddell component has been observed at the bottom of the Brazil basin at around 5°S–4°30S (Andrié et al., 1998; Rhein et al., 1995). Andrié et al. (1998) suggested a pathway of these two components of the AABW at the exit of the Brazil basin: the WSDW component would spread on the western side, while the older, less dense component would instead lie on the eastern side. The characteristics of the bottom water at the entrance of the RFZ seem to indicate that some of the CFM free last component could have turned northeast to feed the RFZ.
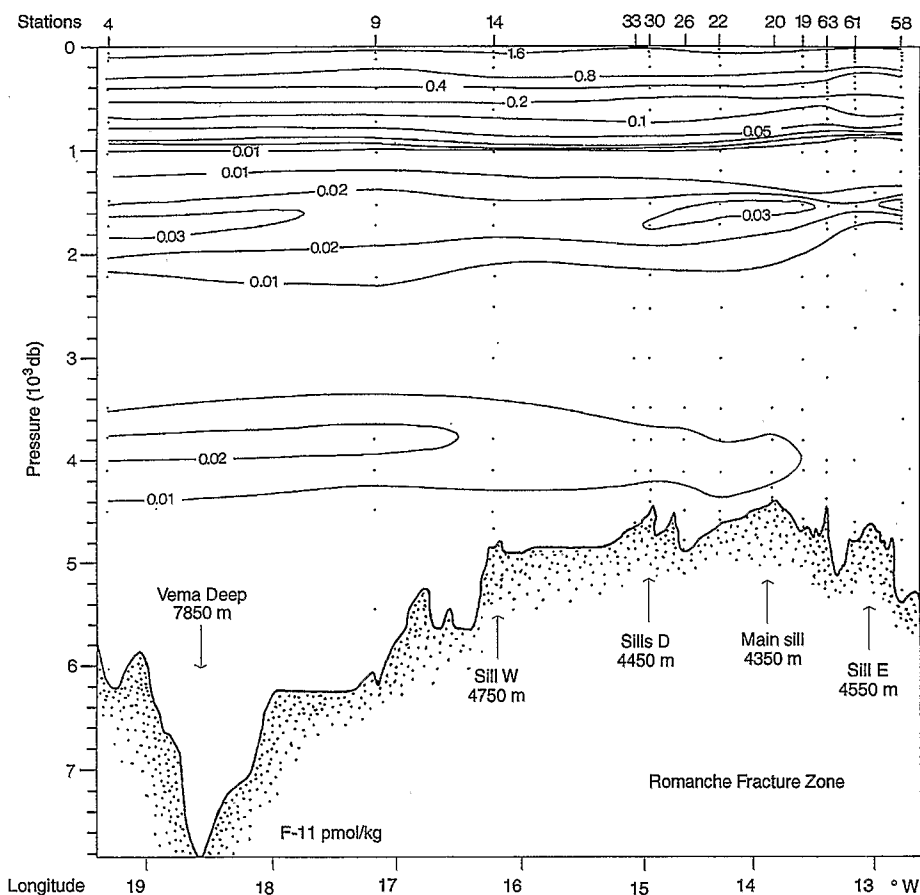

Fig. 5. Deep water section of F-11 (pmol kg^{-1}) versus pressure along the RFZ for August 1991 (Romanche 1). This F-11 section and those following (except Fig. 7) have been hand contoured. Dots show positions of water samples. The smallest F-11 contour intervals are close to the precision of the measurements. See Fig. 2 for station positions.

3.2. Vertical sections

The sections of dissolved F-11 concentrations in the Romanche and the Chain Fracture Zones during the Romanche 1 cruise (August 1991) and Romanche 2 cruise (November 1992) are displayed in Figs. 5–9. A temporal variability of the CFM maxima concentrations is noticeable when the Romanche 1 with the Romanche
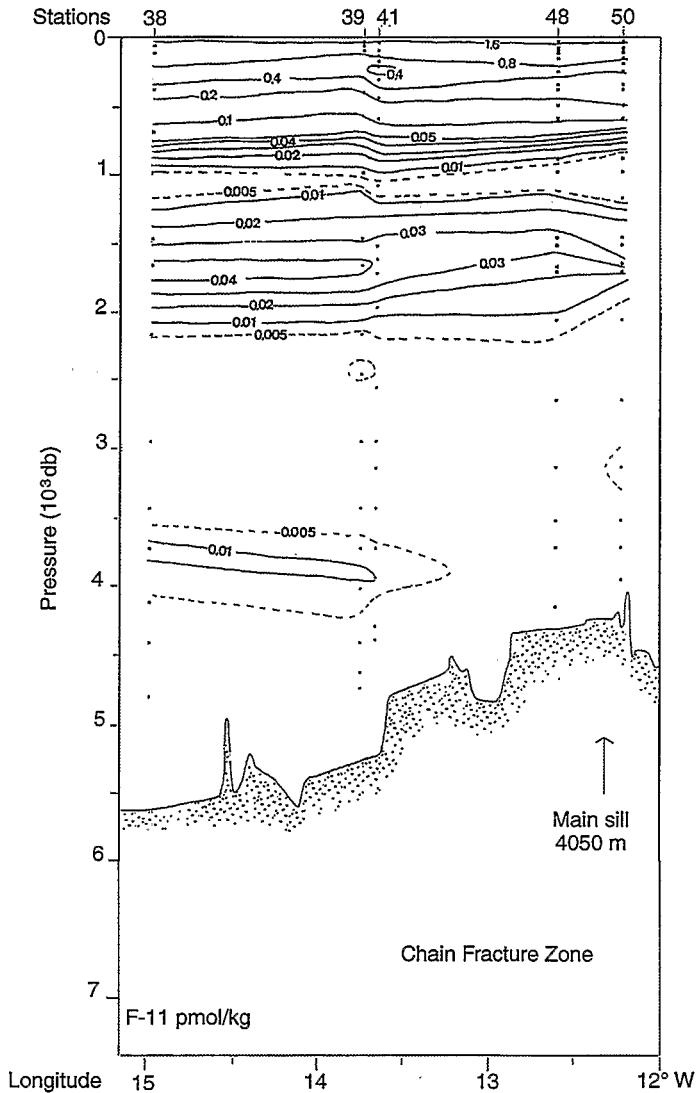

Fig. 6. Deep water section of F-11 (pmol kg^{-1}) versus pressure along the CFZ for August 1991 (Romanche 1), as in Fig. 5.

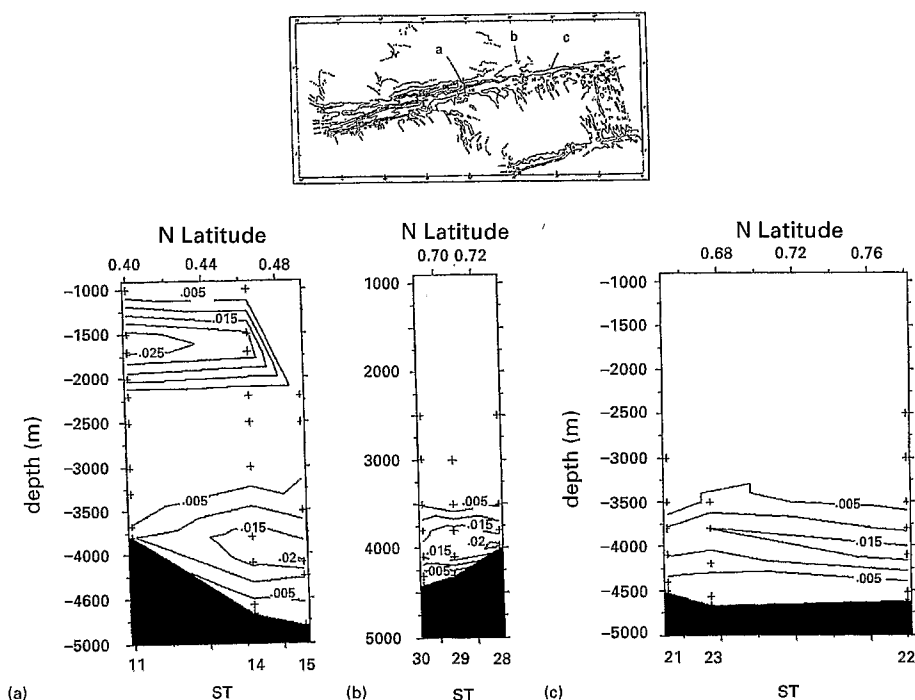Fig. 7. Meridional deep-water sections of F-11 (pmol kg^{-1}) versus pressure across the RFZ realized at (a) 16°W, (b) 15°W and (c) 14°W during August 1991 (Romanche 1), as in Fig. 5.

2 sections along the RFZ (Figs. 5 and 9) are compared. The F-11 profiles below 500 m depth for the station reoccupied during Romanche 2 are presented in Fig. 10. The concentrations measured during the Romanche 2 cruise always appear equal to or higher than the concentrations measured during Romanche 1. The mean increase of the LNADW F-11 maximum is around 0.01 pmol kg^{-1}. At the level of the UNADW, the F-11 increase between the two cruises appears to be larger, with concentration differences reaching 0.05 pmol kg^{-1}.

The F-11 distributions along the RFZ and CFZ show the upper and lower F-11 NADW cores extending eastwards in a CFM-free deep ocean (Figs. 5, 6 and 9). The lower core, constrained by the topography, forms a plume, which decreases eastward in the two fractures, suggesting a transport from west to east. The LNADW F-11 values are stronger in the RFZ (19°W–0.45°S) than the CFZ (15°W–1.5°S), which is farther southeast from the source. This observation can also be associated with the large-scale meridional gradient observed in other tracer distributions upstream of the fracture zones at 25°W (Tsuchiya et al., 1994). Fig. 8, drawn from the Romanche 2 measurements, is the meridional section (3°S–5°N) through both the RFZ (15°W) and the CFZ (13°50′W): the F-11 LNADW signal presents a southward decrease from the RFZ, where levels as high as 0.03 pmol kg^{-1} are observed (whereas in the CFZ the
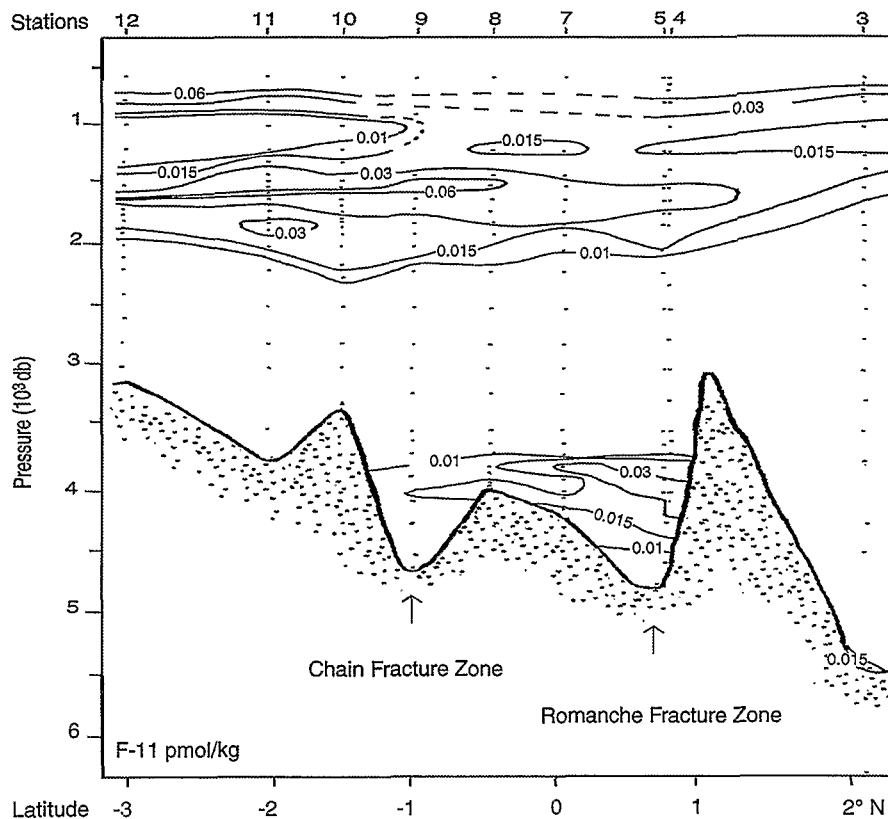
Fig. 8. Meridional deep water section of F-11 (pmol kg^{-1}) versus pressure across the RFZ and CFZ near 14°W for November 1992 (Romanche 2), as in Fig. 5.

levels are less than 0.02 pmol kg^{-1}). These meridional F-11 gradients seem principally to reflect the gradients at the entrances of the fracture zones. Along the RFZ valley (Fig. 5), the LNADW F-11 signal during the Romanche 1 cruise appears affected at the first sill of 4750 m depth (sill W) decreasing below 0.02 pmol kg^{-1}. After the main sill (4350 m), the signal is not detectable in the Romanche 1 data. The F-11 distribution across the RFZ can be visualized in three cross channel sections (Fig. 7) in the RFZ, at 16°W, 15°W and 14°W, respectively. The F-11 lower core seems to be slightly intensified at the RFZ northern wall although the resolution is too coarse to ascertain that feature. Note that this feature is observed right from 16°W before the RFZ south wall vanishes and where it should not be linked to these numerous gaps. In the CFZ (Fig. 6), the F-11 signal decreases below the detection limit at station 48 before the main sill. In the deep valleys of the communication region (not shown), some faint scattered F-11 signals (around 0.01 pmol kg^{-1}) were measured at stations 46, 54, 44 and 57 around 4200, 3800, 4750 and 4400 m depths, respectively, suggesting an influence of recently ventilated LNADW. According to Mercier et al. (1994),
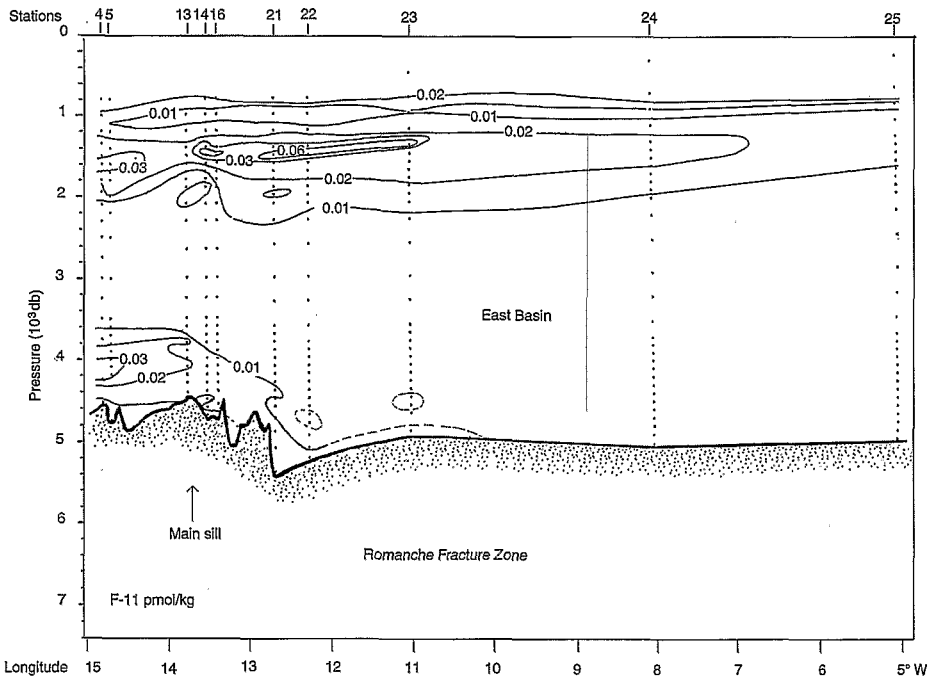
Fig. 9. Deep water section of F-11 (pmol kg^{-1}) versus pressure along the RFZ axis from the sill region into the Guinea basin for November 1992 (Romanche 2), as in Fig. 5.

topographic blocking by the main sill (4050 m) along the valley of the CFZ affects the bottom water and marginally affects the LNADW. However the coldest bottom water blocked by the CFZ main sill most likely enters the communication region whose sills are deeper (4200 m) than the CFZ main sill. Mercier et al. (1994) added that the breaking of the RFZ southern wall favors lateral mixing of the LNADW with the Deep Water of the communication region. The increase of the LNADW F-11 signal between Romanche 1 and Romanche 2 and a fine vertical and horizontal data resolution have allowed us to follow the evolution of the lower F-11 maximum during Romanche 2 along the RFZ valley toward the Guinea Basin and northeast into the Sierra Leone Basin. Mercier et al. (1994) showed that both basins are fed by bottom water following two distinct pathways after a branching, occurring at about 13°12′W. In Fig. 8, the bottom F-11 signal visible around 2°N (Sta. 3) corresponds to the northern exit feeding the Sierra Leone Basin, whereas the F-11 signal within the axis of the RFZ feeds the Guinea Basin. The section along the RFZ channel (Fig. 9) shows that the F-11 maximum is affected while crossing the sills as in the Romanche 1 observations, with values decreasing by 0.02 pmol kg^{-1} between Stations 4, 5 and 14. The F-11 maximum located between 3600 and 4300 m (2.4°C/1.5°C) within the RFZ deepens abruptly towards the eastern basin after passing over the main sill. Using the High-Resolution Profiler, Polzin et al. (1996) showed that the bottom water flow
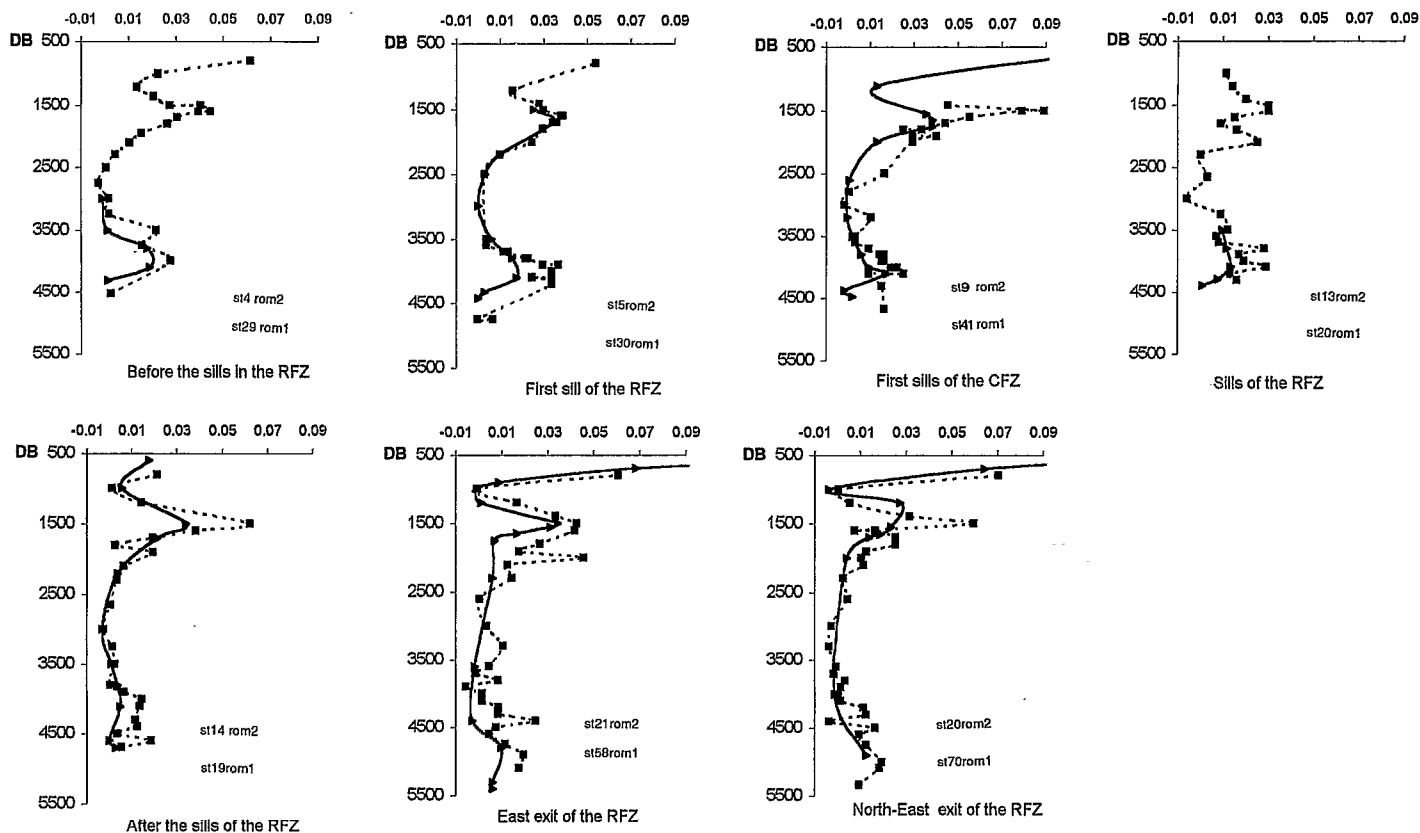
Fig. 10. Comparison of vertical F-11 (pmol kg^{-1}) profiles below 500 dbar measured at the same position in August 1991 (Romanche 1 – solid line) and in November 1992 (Romanche 2 – dashed line).

accelerates downstream of the RFZ main sill, becomes unstable, and feeds intense turbulence, which implies vertical mixing between CFM-free and CFM loaded waters and could explain the observed pertubated tracer signal of the outflow. In the Guinea abyssal plain, the F-11 maximum was found between 4500 m and the bottom within the densest water ($1.45°/1.65°C$). The F-11 concentration weakens eastward and seems to decrease below the detection limit at about 11°W from the Romanche data set. More recently in early 1995, evidence of the eastward invasion of the anthropogenic transient tracer in the Guinea Basin was detected at 9°W (Messias and Mémery, 1998). Along the pathway toward the Sierra Leone Basin, we followed the F-11 maximum up to 2°N. Stations 18–20 along 12°W (not shown) through the northern exit present concentrations around 0.015 pmol kg^{-1}, which are also at greater depths (4700, 4870 and 5088 m) than within the RFZ. This observation suggests that intense mixing also occurs on the pathway toward the Sierra Leone Basin, where Polzin et al. (1996) found evidence for a boundary current.

The UNADW F-11 core was present at all the stations during both Romanche surveys (up to 5°W). Both data sets (Figs. 5, 6 and 8) confirm the southern position (relative to the equator) of the UNADW maxima for both summer and winter seasons. The meridional section (3°S–5°N) crossing the RFZ and the CFZ locates this maximum (values higher than 0.06 pmol kg^{-1}) between 0°5S (1500 m) and 3°S (1600 m). The same indication of a southern shift of the CFM maximum is noted by Doney and Bullister (1992) at 28°W and by Rhein et al. (1995) and Andrié et al. (1998) at 35°W. Tsuchiya et al. (1994) also present a similar shift of the UNADW salinity maximum at 25°W. Andrié et al. (1998) attribute this shift to the eastward bifurcation induced by the rise, around 2000 m depth, of the Parnaiba ridge near 3°S at the western boundary. Two other interesting features of the UNADW found in both Romanche surveys are the presence of lenses of high F-11 concentration and a constriction of the tongue near 13–14°W (Fig. 5 and 9).

4. The shallow CFM maximum

Fig. 11 shows F-11, oxygen and salinity versus $\sigma_{1.5}$ between 950 and 3050 m depth. The oxygen maximum is centered at 2000 m ($\sigma_{1.5} = 34.7$ kg m^{-3}), whereas the CFM and salinity maxima are shallower, between 1600 and 1700 m ($\sigma_{1.5} = 34.63$ kg m^{-3}). The difference in depth of the CFM and oxygen maxima was previously observed along the DWBC to the north (Pickart, 1992) and in the equatorial Atlantic (Weiss et al., 1985; Molinari et al., 1992; Rhein et al., 1995). Several explanations have been given in the literature. At 40°N, Pickart (1992) observed that the oxygen content of the UNADW is reduced by consumption and vertical mixing with low oxygen water lying above. Rhein et al. (1995) add that this water mass, located around 600–700 m in the northern Atlantic, has a higher oxygen consumption than deeper water masses. Rhein et al. (1995) also suggest that convection to 500 m depth, which occurs for the UNADW (Talley and McCartney, 1982; Pickart, 1992), would produce higher CFM concentrations compared to convection to 2000 m depth, which occurs for the classical LSW (Gascard and Clarke, 1983). Note that incomplete
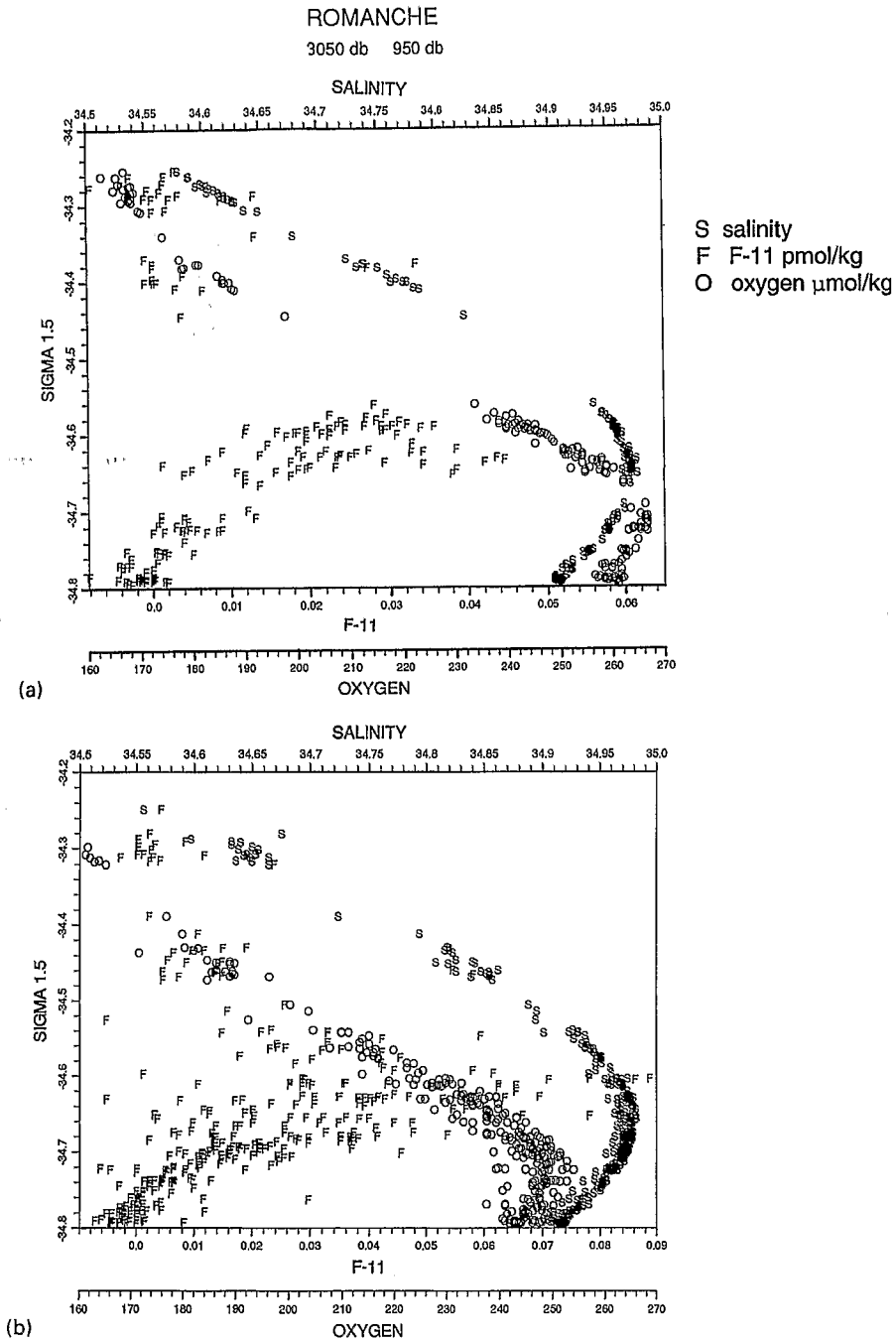
ROMANCHE

3050 db   950 db

(a)

(b)

Fig. 11. F-11 (pmol kg^{-1}), salinity and oxygen (μmol kg^{-1}) versus $\sigma_{1.5}$ (34.2–34.8) for (a) Romanche 1 stations and (b) Romanche 2 stations.
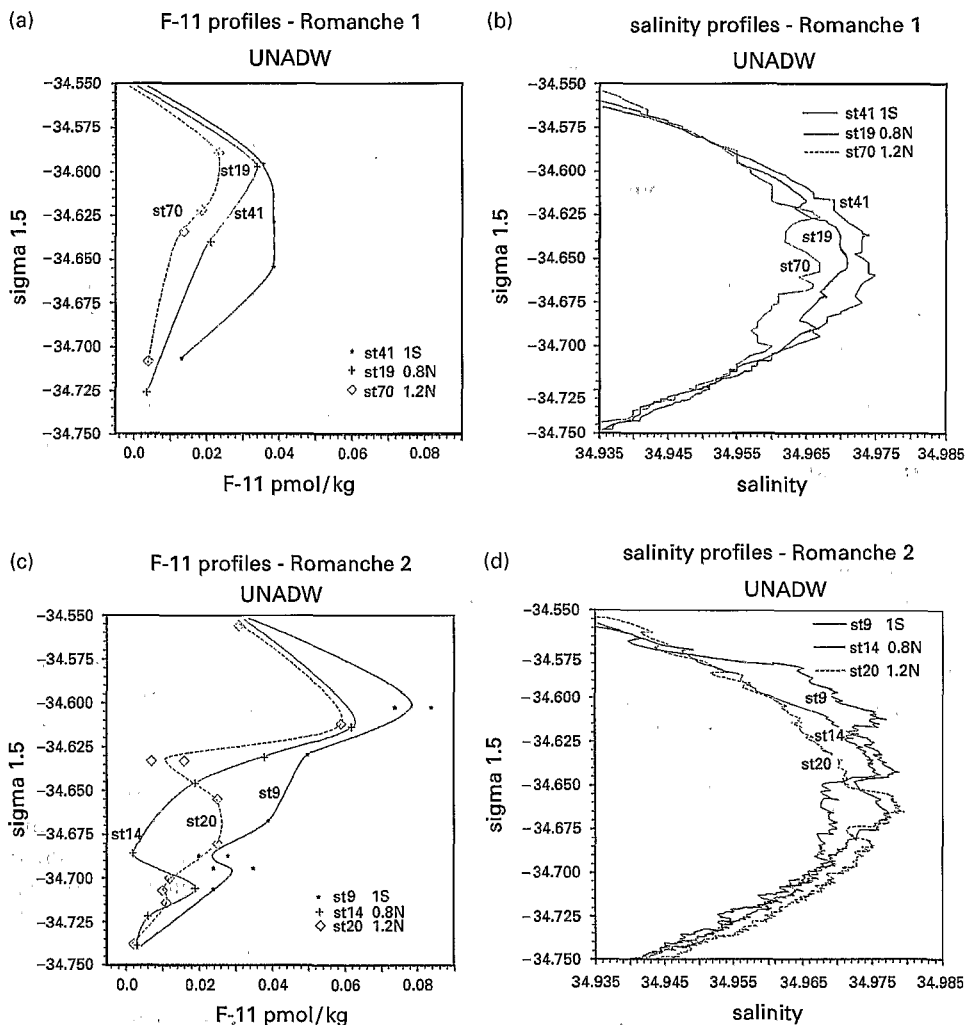
Fig. 12. Profiles of F-11 (pmol kg^{-1}) and salinity versus $\sigma_{1.5}$ (34.55–34.75) for (a, b) Romanche 1 stations 70, 19 and 41 and (c, d) Romanche 2 stations 20, 14 and 9 made at the same position.

convection during the 1960s and 1970s could have also produced low CFM LSW (Lazier, 1988).

The CFM and salinity distributions show features that are strikingly correlated (Fig. 11). During the Romanche 1 cruise, we observed a variability of the depth of the CFM maxima, which were found between 1400 and 1900 m (Figs. 12a/d). The southern (37, 38, 41) and western (4) stations present regular, well-defined maxima in CFM and salinity at the same depth near 1700 m (see for example Fig. 12a and b, station 41). In contrast, to the northeast of the studied region (stations 70, 58), the F-11 maximum

(near 1550 m) seems truncated from below (see for example Fig. 12a and b, station 70). Simultaneously, the corresponding salinity profiles are diminished and pertubed. This suggests the influence of a water mass with lower CFM and salinity in the northeastern region of the RFZ at the density of $\sigma_{1.5} = 34.65$. Station 19 shows the intermediate situation. We observe an increase both in the salinity and the F-11 concentrations between Romanche 1 and Romanche 2 cruises (Fig. 11). This increase is clearly seen by comparing profiles (Fig. 12a–d) of the stations done at the same position during the two cruises (0.012 in salinity and 0.03 pmol kg^{-1} in F-11 relative to station 70 of Romanche 1). In the Romanche 2 data, the upper CFM signal in the northeast of the region is split into two maxima separated by slight minima at 1600 m depth. The high salinity of the upper CFM core can result from double diffusive mixing with the overlying water of Mediterranean origin (Sarmiento, 1986). Böning and Schott (1993) show a map of the salinity tongue at the 1500 m depth flowing parallel to the equator (their Fig. 1). The salinity gradient observed in this map in the N-E zone of the Romanche 1 area could be responsible for the variability of the Romanche salinity profiles. Another explanation suggested by the particular feature of the upper transient tracer signal could be as follows. The lateral distribution of CFMs shows zones of alternating high and low concentration extrema in the most northeastern stations. This distribution of the high F-11 lenses seems to indicate that the upper CFM signal is not monotonically transported eastward along the equator. One possible mode of transport is by non-stationary currents or jets (horizontal mixing). A vertical profile of velocities measured on 17 January 1989 in the equatorial Atlantic (0°00′N, 30°22′W) reveals westward flows from 1400 to 1600 m and eastward flows between 1600 and 2200 m (Ponte et al., 1990). SOFAR float data at nominal depths of 1800 m (Richardson and Schmitz, 1993) show the presence of reversing equatorial currents with timescales of the order of 18 months. Richardson and Schmitz (1993) found an eastward equatorial current followed a year later by a reversing westward equatorial current. They suggest that this could have advected the observed F-11 tongue to the east along the equator. The high variability of the F-11 profiles that we found can result from the effects of these reversing flows in the north of the main CFM core. The model calculations of Böning and Schott (1993) yielded seasonally reversing eastward and westward transport with only a small mean annual eastward transport. Böning and Schott (1993) add that the latter was sufficient to maintain the salinity tongue. The temporary westward current may perhaps diminish the spreading of the transient tracers and in particular CFMs (see Section 6).

5. The deep CFM maximum

Two elements can explain the dramatic decrease of the F-11 signal in the RFZ: the transient behavior of the CFM and the dilution by lateral and vertical mixing. Direct current measurements in the fracture zone have shown permanent and important eastward velocities (Polzin et al., 1996; Mercier and Speer, 1997). Due to the very short transit time for fluid parcels within the RFZ, transient effects should not be important in establishing the zonal gradient. As seen in Section 3.1, the deep CFC maximum
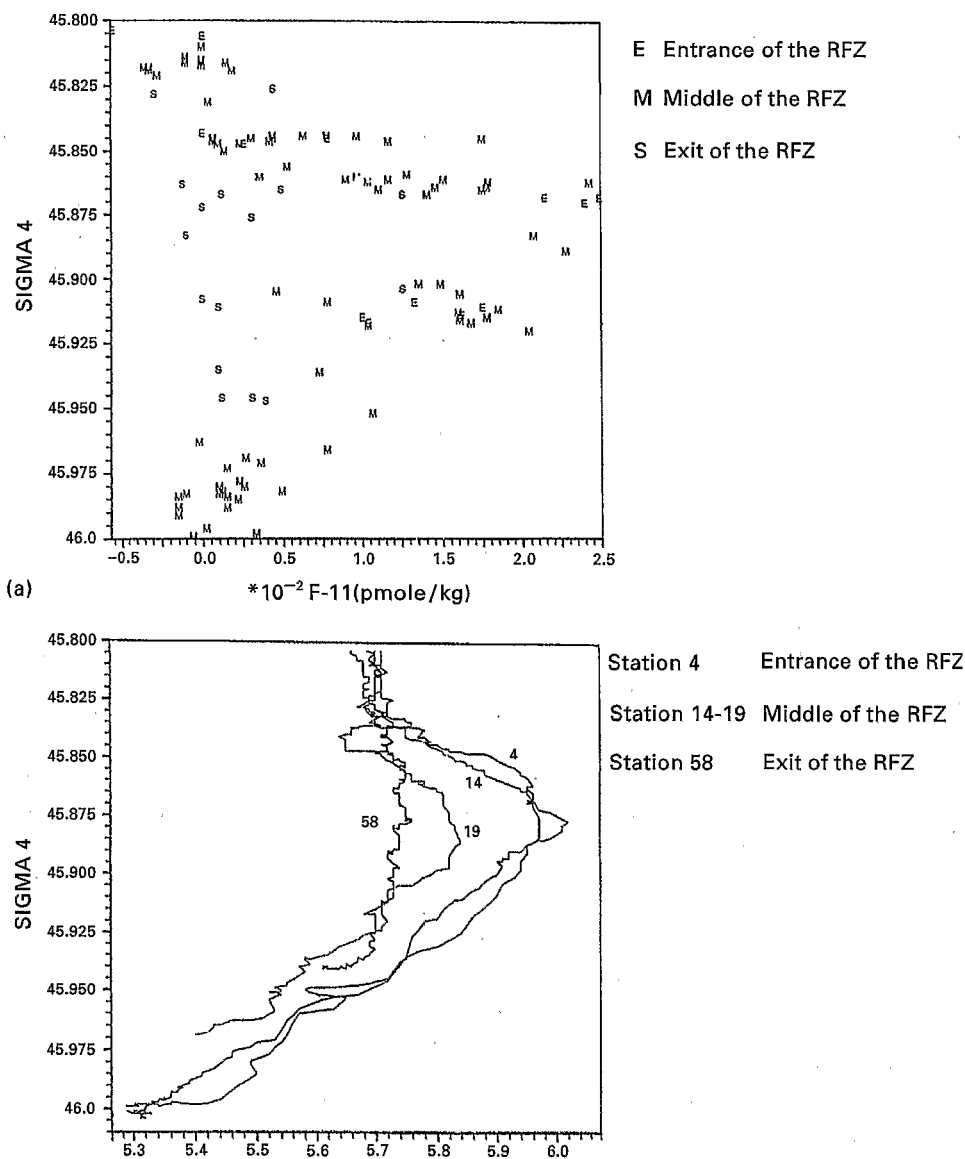
(a)

E Entrance of the RFZ

M Middle of the RFZ

S Exit of the RFZ

Station 4   Entrance of the RFZ

Station 14-19 Middle of the RFZ

Station 58   Exit of the RFZ

Fig. 13. Evolution of the (a) F-11 (pmol kg^{-1}) and (b) oxygen (ml l^{-1}) deep maxima versus σ_4 (45.8–46) along the RFZ from Romanche 1 cruise.

used to trace the LNADW is associated with an oxygen maximum at the entrances of both fracture zones (initial density between $\sigma_4 = 45.85$ and 45.95). Comparison of the oxygen and the F-11 signal along the RFZ and the CFZ shows that the two tracer maxima have a similar evolution (Fig. 13a and b), decreasing through the sills. At the eastern exit of the RFZ, the oxygen and F-11 profiles below 3500 m are

relatively homogenous (station 58, Fig. 13b). In Fig. 14, we observe a simple linear trend between F-11 and oxygen characteristics for deep waters. After the sills, the F-11 – oxygen correlation is no longer evident due to the low F-11 concentrations (Fig. 14b). In the eastern basin, the lower CFM signal is weaker in oxygen and also colder, deeper, less salty and richer in nutrients than at the entrance of the channel, giving evidence of the AABW influence. The coldest and purest bottom water used to trace the AABW, shown in Fig. 15, has undetectable values in F-11 within the RFZ. The anticorrelated hydrographic characteristic changes in the LNADW compared to the AABW supports the idea that vertical mixing is the primary mechanism for the modification of both water masses through the RFZ sills, in agreement with the findings of Polzin et al. (1996) and Ferron et al. (1998), who inferred highly efficient vertical mixing and averaged diapycnal diffusion coefficients of $150 \, \mathrm{cm^2 \, s^{-1}}$ with maximum values as large as $0.1 \, \mathrm{m^2 \, s^{-1}}$ downstream of the Romanche Fracture Zone main sill.

6. Apparent ages and dilution factors

Based on the continuous increase from 1931 until the mid-1970s of the F-11 : F-12 ratio in the atmosphere, we can estimate the date at which a water parcel became isolated from its source region by its F-11 : F-12 concentration ratio (Fig. 16). The apparent age of the water sample is then defined as the time difference between the year corresponding to the original atmospheric ratio of the water sample and the date of the sampling. We follow the method of Weiss et al. (1985): the original atmospheric ratio is computed from the sample F-11 and F-12 concentrations using solubility functions (Warner and Weiss, 1985). The estimated precision and accuracy of the CFM solubility functions are ~0.7 and 1.5%, respectively. The source water is assumed to be in approximate solubility equilibrium with the atmosphere. We have computed the apparent ages for the UNADW and the LNADW CFM cores using the northern hemisphere 1931–1990 input function as provided to us by Weiss (personal communication, 1992). The method assumes that mixing occurs with CFM-free water so that the F-11 : F-12 ratio is not altered by mixing after the water parcel becomes isolated from the source region. In reality, the residence time of the water mass in its formation area or mixing with water loaded in CFM tends to lower the F-11 : F-12 ratio and leads to an overestimation of the apparent age (Pickart et al., 1989). The two CFM tongues observed in the Romanche area are surrounded by CFM-free waters. But, mixing with water loaded with CFMs could have occurred upstream, notably in the DWBC (with adjacent water accumulating CFMs, see Pickart et al., 1989). In the present study, no correction of the F-11 : F-12 ratio relative to these processes was made and the computed age estimates are an upper bound of the true age. A dilution factor is derived by dividing the CFM source surface water concentration at the time of formation inferred from the apparent age by the observed CFM concentration. The dilution factor critically depends on the water mass source saturation. Equilibrium between atmosphere and ocean is not always achieved in deep water formation regimes, affecting the CFM concentration of newly formed deep water (Rhein, 1994).
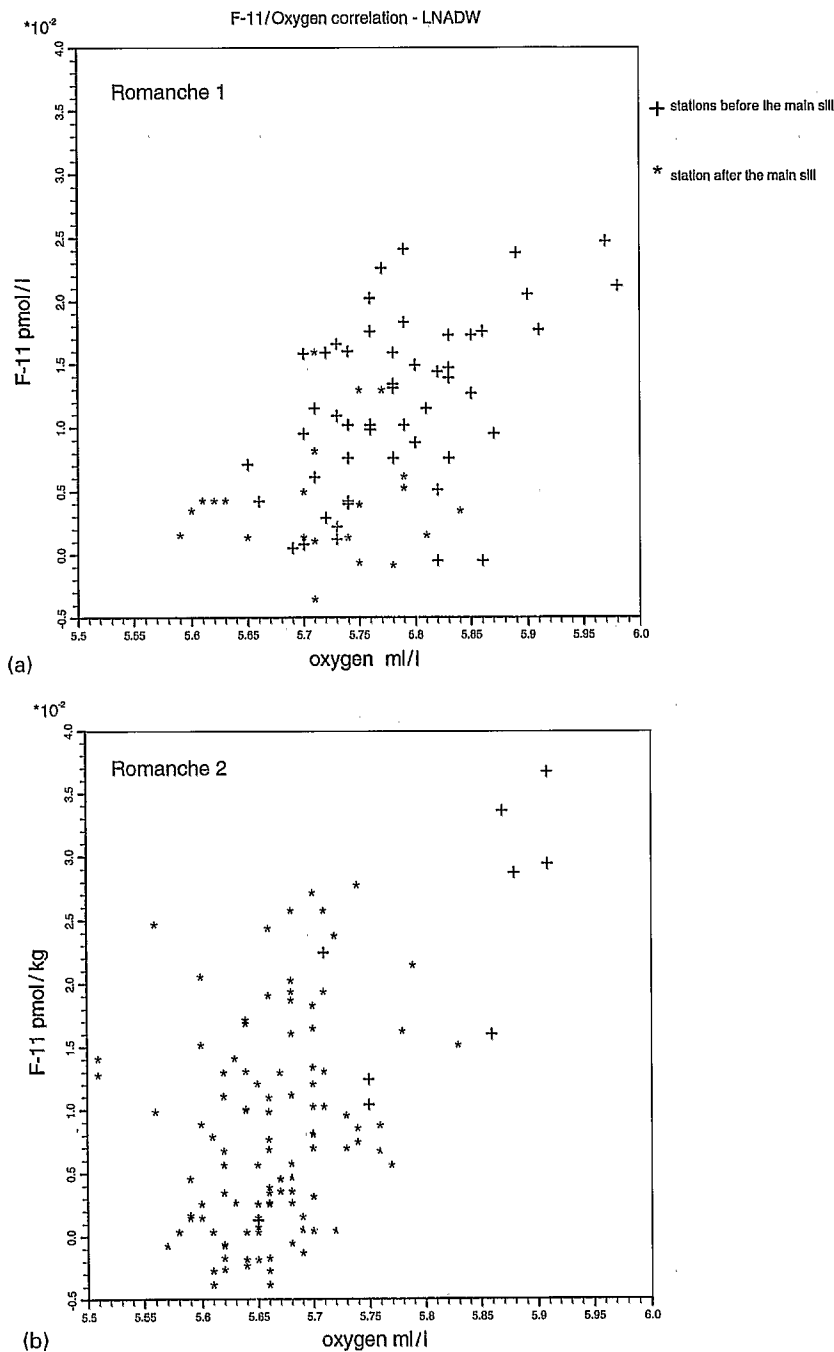
Fig. 14. F-11 (pmol kg^{-1}) versus oxygen (ml l^{-1}) for water samples below 3000 dbar in the RFZ for (a) Romanche 1 stations and (b) Romanche 2 stations. Stars represent stations located at the exit of the sills.
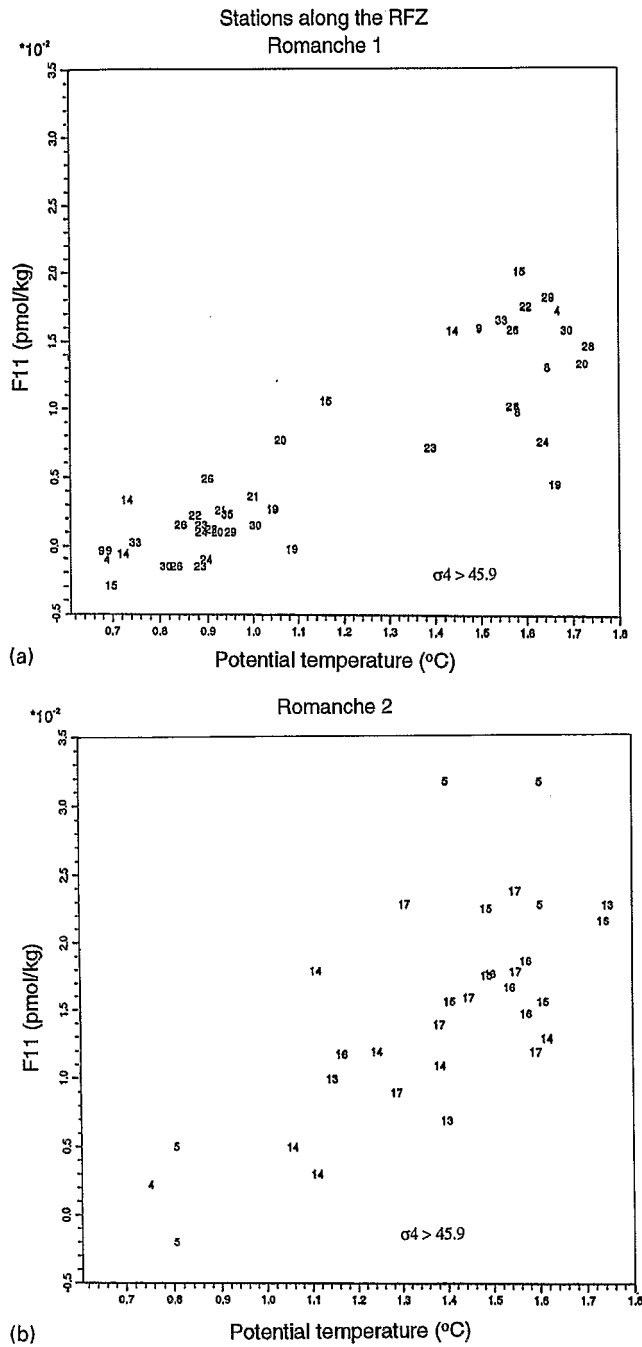
Fig. 15. F-11 (pmol kg^{-1}) versus potential temperature (°C) for bottom water samples ($\sigma_4 > 45.9$) for (a) Romanche 1 stations and (b) Romanche 2 stations. Station numbers are plotted at the F-11/potential temperature points.
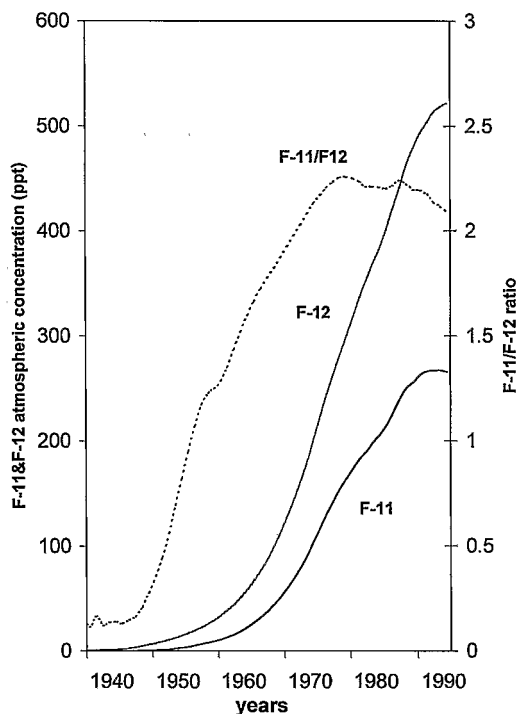
Fig. 16. F-11 to F-12 concentration ratio in the assumed DSOW source surface waters. The curve represents values for water of − 0.5°C and 34.8 (for upper AAIW; Smethie, 1993) in equilibrium (Warner and Weiss, 1985) with reconstructed atmospheric concentrations in the Northern Hemisphere.

Saturations of only 60% have been reported, for example, in the case of the newly formed LSW (Wallace and Lazier, 1988). Therefore, the observed concentrations give a lower value of dilution (Weiss et al., 1985; Pickart et al., 1989). A limitation in the Romanche study is the very low CFM concentrations that lead to large errors in the F-11:F-12 ratio (ranging from 10% for F-11 = 0.06 pmol kg^{-1} to 100% for values below 0.015 pmol kg^{-1}), which leads to even larger uncertainties for the derived parameters.

In Fig. 17, we report the apparent age versus the F-11:F-12 ratio calculated for the Romanche 1 and Romanche 2 stations. For the UNADW, the results are relatively homogenous. The calculated atmospheric F-11:F-12 ratio of the UNADW (average for each station) ranges from 1.65 to 2. It is characteristic of surface waters from 1966 to 1972 and implies a mean travel time from the source region to the RFZ of around 25 ± 4 years. Mean dilution factors for Romanche 1 and Romanche 2 are 27 ± 10 and 36 ± 12, respectively, for the transient tracer compounds in this layer. The values of the apparent age obtained are consistent with values previously inferred from CFMs along the DWBC in the literature, which increase in the downstream direction (Table 1a). Smethie (1993) gave an apparent age for the UNADW of ∼11 years at
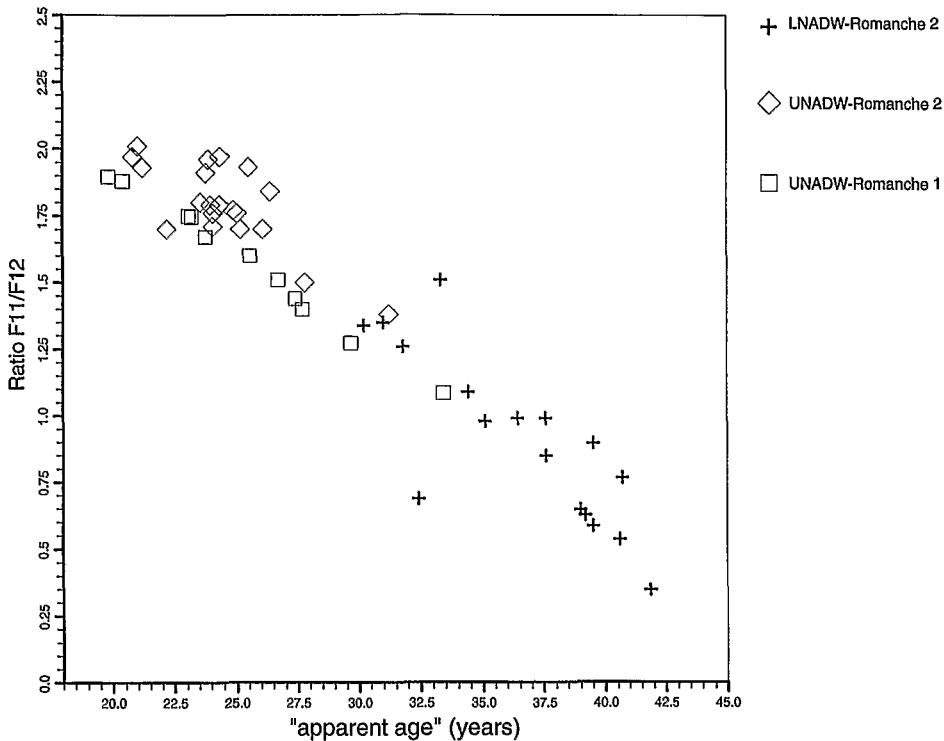
Fig. 17. F-11 : F-12 ratio versus apparent age calculated for the deep CFM maxima from Romanche 1 (only for the UNADW: on the Romanche 1 cruise, contamination problems precluded the use of the F-12 data on station 4–39) and Romanche 2 (UNADW and LNADW). The symbol codes are (+) for the UNADW CFM maximum and (∗) for the LNADW CFM maximum.

44°N and ∼18 years at 33°N. Further south, the values reach ∼20 years at 7.3°N (Andrié et al., 1997) and ∼23 years at the equator (Weiss et al., 1985). The F-11 value of the upper core was found to be diluted by a factor of 5 at the equator in 1983 (Weiss et al., 1985). Andrié et al. (1998) estimated dilution factors ranging from 8 ± 1 at 7°30′N within the DWBC to around 50 ± 30 at 3°5′W in the equatorial eastern Atlantic. Rhein et al. (1995) reported a dilution factor of 29 before the water reaches the equator. The high dilution factor in the UNADW along the equator may reflect the effects of time- dependent reversing equatorial currents or jets (Richardson and Schmitz, 1993) discussed above (Section 4). These flows advect the CFM tongue eastward into the surrounding CFM free water, but also return westward, increasing the mixing of the transient tracer compounds in this layer. In the present work, the LNADW CFM core appears significantly older but less dilute than the UNADW core. The F-11/F-12 ratios measured in the LNADW core range from 0.6 to 1.5, giving an average apparent age of $\sim 36 \pm 5$ years and a dilution of 10 ± 5. These values are consistent with previous CFC-based estimates in the DWBC further north (Table 1b)

Table 1
Comparison of the properties for (a) the upper CFM maximum and (b) the lower CFM maximum, obtained from the Romanche cruises and from previous cruises upstream of the RFZ along the DWBC

Cruise & Reference	Position	F11 pmol kg^{-1}	F11/F12 Ratio	Ratio Date	Ratio Age (years)	Dilution Factor	Distance from source (km)	Apparent mean Current speed (cm.s^{-1})
(a) *Properties of the upper CFC maximum from different cruises*								
1991 Romanche 1, present work	Equ. 16'W	0.03	1.7	1965	26	27	11 500	1.4
1992 Romanche 2, present work	Equ. 16°W	0.06	1.8	1967	25	36	11 500	1.3
1993 WHP-A6, Andrié et al. (1995)	DWBC 7°30'N	> 0.32	—	—	< 20	8	—	—
1982–83 TAS, Weiss et al. (1985)	Equ. 50–30°W	0.05	1.4	1963	25	5	10 000	1.4
1986 WBEX, Smethie (1993)	DWBC 33°N	0.77	1.88	1968	18	1.8	5400	0.8
1983 OCE-134, Smethie (1993)	DWBC 44°N	1.54	2.1	1972	11	1.5	2300	0.65
(b) *Properties of the lower CFC maximum from different cruises*								
1992 Romanche 2, present work	Equ.-16'W	0.03	0.96	1956	36	5–15[a] to 20/40 after the sills	13 000	1.2[b]
1986 WBEX, Smethie (1993)	DWBC 33'N	0.40	1.74	1966	20	> 2	7710	1.2[b]
1983 OCE-134, Smethie (1993)	DWBC 44°N	0.63	1.86	1968	15	> 2	5400	1.1[b]

[a] Doney and Jenkins (1994) calculated a dilution factor of about 16 (8–32) at 20°N for the LNADW using TTO Tritium-3He data in a simple boundary current/abyssal ventilation model for the western basin of the North Atlantic.

[b] Pickart et al. (1989) have shown how mixing can reduce the F11 : F12 ratio in the core of the DWBC. Assuming that CFM-free mixing occurs in the current and that the CFM ratio is not altered during deep water formation and overflow, the predicted core speed from the F11/F12 ratio, was 2 cm s^{-1}. Modeling the DWBC by simple advective–diffusive boundary current models coupled to a convection model of the Iceland–Scotland overflow, Pickart et al. (1989) obtained core speeds of 5–10 cm s^{-1} for the DWBC from matching model solutions to CFM data collected along the western boundary. These values are of the same order of magnitude as DWBC velocities observed with current meters, generally 5–7 cm s^{-1} south of the Grand Banks (Watts, 1991). Using the ideas of Pickart et al. (1989), Rhein (1994) obtained by modeling transient tracer a mean velocity of 4.8 cm s^{-1} for the DWBC south of the Faroe Bank to 10°S.
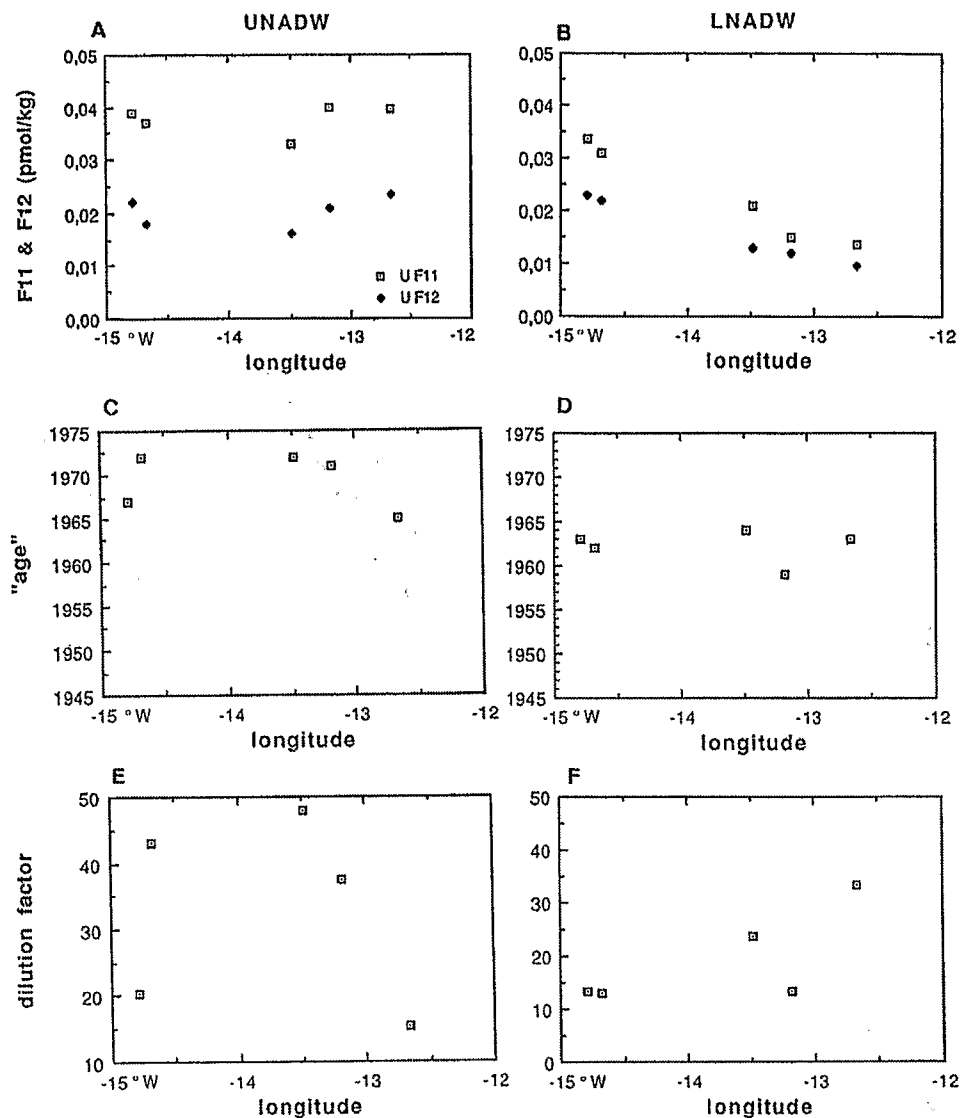
Fig. 18. F-12 and F-11- concentrations (pmol kg^{-1}), apparent ages and dilution factors calculated from the F-11:F-12 ratio versus longitude along the RFZ axis for the upper CFM maximum (a, c, e) and the lower CFM maximum (b, d, f).

as well as with a dilution factor of about 16 (8–32) calculated by Doney and Jenkins (1994) at 20°N using TTO Tritium-^{3}He. Compared to the UNADW core, the low LNADW dilution factor (~ 10 found within the RFZ before the sills) suggests a more steady flow guided by the topography that limits mixing with CFM-free water. Dilution factors increase to around 30 ± 20 beyond the sills. In Fig. 18, we have

reported the F-11 and F-12 concentrations, the apparent age and the dilution factor along the RFZ for the LNADW and the UNADW. We use only stations along the RFZ axis with well-defined CFM maxima. The dramatic decrease of the LNADW CFM concentration along the fracture axis is not linked to the age of the water, which stays constant. In contrast, the dilution factor increases from the west to the east. Hence, the decrease of the CFM concentration appears to be mainly the result of mixing by dilution with CFM-free water rather than the result of the transient behavior of the CFMs. However, the very low concentration of CFMs in the LNADW implies an error close to 100% in the ratio F-11 : F-12 and raises concerns about the possibility of estimating the transient behavior.

The apparent mean current speed has been calculated from the F-11 : F-12 ratio apparent age and the distance from the source. The travel time of about 25 years from the Labrador Sea source and 35 years from the Nordic Seas to the Romanche area indicates mean apparent velocities of 1.4–1.3 cm s^{-1} for the UNADW and 1.2 cm s^{-1} for the LNADW. These values fall in the range of previous estimates for the NADW in the DWBC or along the equator based on CFMs (Table 1) and Tritium-^{3}He estimates (on the order of 0.75–1.5 cm s^{-1}, Doney and Jenkins, 1994) but are significantly smaller than those measured using direct methods. The interpretation of the tracer-based velocity estimates has been much discussed in recent years (Pickart et al., 1989, McCartney, 1993; Smethie Jr., 1993, Doney and Jenkins, 1994). Mean spreading rates estimated with transient tracers include the effects of mixing and recirculation with the alongstream advection along the travel path and lead to a lower limit. CFM modeling experiments (Pickart et al., 1989; Rhein, 1994) also indicate that the earlier assumptions of CFM core mixing with CFM-loaded water could cause the estimated speed to be underestimated (Table 1).

7. Summary and concluding remarks

Chlorofluoromethanes have been measured in the deep water in the Romanche and Chain Fracture Zones in the equatorial Atlantic during two surveys, in August 1991 and November 1992. These two openings in the Mid-Atlantic Ridge allow deep water exchanges between the western and eastern basins. The identification of the eastward spreading of two NADW CFM signals (at depths of 1600 and 3800 m) originating from the DWBC confirms the earlier interpretation of Weiss et al. (1985) and Doney and Bullister (1992) regarding a splitting at the DWBC near the equator. One of the most interesting results of this work is the evidence of the lower CFM signal (LNADW) penetrating the Romanche (19°W–0.45°S) and the Chain (15°W–1.5°S) Fracture Zones.

The upper CFM maximum (UNADW) appears south of the Equator and was followed eastward as far as 5°W–1.45°N. The equatorial UNADW F-11 core was more recently intersected at 3°5'W in January 1993 (Andrié et al., 1998) and 2°W in January 1995 (Messias and Mémery, 1998). In particular, on the meridional section along 2°W, south of the main equatorial UNADW core, scattered CFC lenses were

visible until 12°S, giving some evidence for a southward flow of the UNADW from the equatorial region along the eastern boundary (Messias and Mémery, 1998).

The concentration of the lower CFM maximum found in the fracture zone is in agreement with the suggestion that the splitting of the LNADW at the DWBC explains the north–south CFM gradient observed at the equator (between 5°N and 5°S) as pointed out by Rhein et al. (1995) and Andrié et al. (1998). The lower CFM core evolution within the fracture zones appears to be closely related to the topography. The LNADW CFM signal is stronger in the RFZ than in the CFZ and was followed down to the eastern basin. The characteristics of the CFM signals change as they pass the sills of the RFZ, showing clear qualitative transformation of the water mass: the CFM signal decreases and sinks to greater depths in the eastern basins. The observations suggest that a mixture of CFM-loaded LNADW, lateral water and AABW extends down to the bottom, east into the Guinea Basin and northeast into the Sierra Leone Basin. These mixing process have also been seen in the $CTDO_2$ and nutrient data by Mercier et al. (1994) and Mercier and Morin (1997). The CFM data reveal that there is an active ventilation of the eastern basin by waters carrying anthropogenic CFM derived from the Romanche fracture zone. In the deep Angola Basin at 19°S, F-11 and F-12 concentrations were undetectable; however, traces of anthropogenic CCl_4 were found in the bottommost water on the eastern side of the Mid-Atlantic Ridge (Wallace et al., 1994). CCl_4 is a transient tracer with a longer water-dating scale than F-11 and F-12, since it was introduced to the ocean at the beginning of the 20th century. Wallace et al. (1994) suggested the possibility of ventilation of the Angola Basin from the RFZ and through the Walvis Ridge. The agreement with earlier CFM results in the deep equatorial Atlantic ocean encourages the study of the evolution of this transient-tracer signature in the eastern basin.

The attempt to date the UNADW and LNADW CFM core from the F-11/F-12 ratio gives constant mean ages of 25 ± 4 years and 36 ± 5 years, respectively, along the Romanche fracture zone. The UNADW appears to be 'younger' but more dilute (20–40) than the LNADW (5–15), perhaps affected by reversing equatorial currents. The dilution factor of the LNADW CFM core increases through the sills from around 10 to 30. These estimates can be biased because of upstream mixing effects and because of the very low CFM concentrations measured here. The interpretation of these results should therefore be used with caution. A comparison with a numerical model that includes an explicit treatment of circulation and mixing could yield further insights into the apparent age estimates computed here.

References

Andrié, C., Ternon, J.-F., Messias, M.-J., Mémery, L., Bourlès, B., 1998. Chlorofluoromethane distributions in the deep equatorial Atlantic during January–February 1993. Deep-Sea Research I 45, 903–929.

Böning, C.W., Schott, F.A., 1993. Deep currents and the eastward salinity tongue in the Equatorial Atlantic: results from an eddy – resolving, primitive equation model. Journal of Geophysical Research 98, 6991–6999.

Bullister, J.L., 1989. Chlorofluorocarbons as time-dependent tracers in the ocean. Oceanography 2, 12–17.

Doney, S.C., Bullister, J.L. 1992. A chlorofluorocarbon section in the eastern North Atlantic. Deep-Sea Research 39, 1857–1883.

Doney, S.C., Jenkins, W.J., 1994. Ventilation of the deep western boundary current and Abyssal Western North Atlantic: estimates from Tritium and ^{3}He distributions. Journal of Physical Oceanography, 24, 638–659.

Ferron, B., Mercier, H., Speer, K.G., Gargett, A., Polzin, K.L., 1998. Mixing in the Romanche Fracture Zone. Journal of Physical Oceanography 28, 1919–1945.

Fine R.A., Molinari, R.L., 1988. A continuous deep western boundary current between Abaco (26.5°N) and Barbados (13°N). Deep-Sea Research 35, 1441–1450.

Friedrichs, M.A.M., Hall, M.M., 1993. Deep circulation in the tropical North Atlantic. Journal of Marine Research 51, 697–736.

Gascard, J.-C., Clarke, R.A., 1983. The formation of Labrador Sea Water. Part II: mesoscale and smaller-scale processes. Journal of Physical Oceanography 13, 1779–1797.

Heezen, B.C., Bunce, E.T., Hersey, J.B., Tharp, M., 1964. Chain and Romanche Fracture Zones. Deep-Sea Research 11, 11–33.

Lazier, J.R.N., 1988. Temperature and salinity changes in the deep Labrador Sea, 1962–1986. Deep-Sea Research 35, 1247–1253.

Mantyla, A.W., Reid, J.L., 1983. Abyssal characteristics of the World Ocean waters. Deep Sea Research 30, 805–833.

Mauritzen, C.A., 1996. Production of dense overflow waters feeding the North Atlantic across the Greenland-Scotland Ridge. Part 1: evidence for a revised circulation scheme. Deep Sea Research I 43(6) 769–806.

McCartney, M.S., 1993. Crossing of the equator by the deep western boundary current in the western Atlantic Ocean. Journal of Physical Oceanography 23, 1953–1974.

McCartney, M.S., Bennett, S.L., Woodgate-Jones, M.E., 1991. Eastward flow through the Mid-Atlantic Ridge at 11°N and its influence on the abyss of the eastern basin. Journal of Physical Oceanography 21, 1089–1121.

Mercier, H., Billant, A., Branellec, P., Morin, P., Messias, M.J., Mémery, L., Thomas, C., Honnorez, J., 1992. Campagne Romanche 1- Données CTDO$_2$, Chimie et Bathymétrie. Rapport Interne Laboratoire de Physique des Océans 92-02.

Mercier, H., Billant, A., Branellec, P., Andrié, C., Messias, M.J., Gouriou, Y., Laguadec, C., 1995. Campagne Romanche 2- Données de la sonde CTDO$_2$, Mesures de Salinité, d'Oxygène Dissous et des Chloro-fluorométhanes, Courantométrie Acoustique Doppler. Rapport Interne Laboratoire de Physique des Océans 95-02.

Mercier, H., Morin, P., 1997. Hydrography of the Romanche and the chain fractures zones. Journal of Geophysical Research 102, 10,373–10,389.

Mercier, H., Speer, K.G., Honnorez, J., 1994. Flow pathways of bottom water through the Romanche and chain fracture zones. Deep-Sea Research I 41, 1457–1477.

Mercier, H, Morin, P., 1997. Hydrography of the Romanche and chain fracture zones. Journal of Geophysical Research 102, 10,373–10,389.

Mercier, H., Speer, K.G., 1998. Transport of bottom water in the Romanche fracture zone and the chain fracture zone. Journal of Physical Oceanography 28, 779–790.

Messias, M.J., Mémery, L., South Atlantic Chlorofluoromethanes distributions along the WHP lines A17, A13 and A14, WOCE Newsletter, 31, 21–27.

Metclaf, W.G., Heezen, B.C., Stalcup, M.C., 1964. The sill depth of the Mid-Atlantic Ridge in the equatorial region. Deep-Sea Research 11, 1–10.

Molinari, R.L., Fine, R.A., Johns, E., 1992. The deep western boundary current in the tropical North Atlantic ocean. Deep-Sea Research 39, 1967–1984.

Pickart, R.S., 1992. Water mass components of the North Atlantic deep western boundary current. Deep-Sea Research 39, 1553–1572.

Pickart, R.S., Hogg, N.G., Smethie, Jr., W.M., 1989. Determining the strength of the deep western boundary current using Chlorofuoromethane ratio. Journal of Physical Oceanography 19, 940–951.

Polzin, K.L., Speer, K.G., Toole, J.M., Schmitt, R.W., 1996. Intense mixing of Antarctic bottom water in the equatorial Atlantic Ocean. Nature 380, 54–57.

Ponte, R.M., Luyten, J., Richardson, P.L., 1990. Equatorial deep jets in the Atlantic Ocean. Deep-Sea Research 37, 711–713.

Reid, J.L., 1989. On the total geostrophic circulation of the South Atlantic Ocean: flow patterns, tracers, and transports. Progress in Oceanography 23, 149–244.

Reid, J.L., 1994a. On the total geostrophic circulation of the North Atlantic Ocean: flow patterns, tracers, and transports. Progress in Oceanography 33, 1–92.

Rhein, M., 1994b. The deep western boundary current: tracers and velocities. Deep-Sea Research I 41, 263–281.

Rhein M., Stramma, L., Send, U., 1995. The Atlantic deep western boundary current: water masses and transports near the equator. Journal of Geophysical Research 100, 2441–2457.

Richardson, P.L., Schmitz, Jr., W.J., 1993. Deep cross-equatorial flow in the Atlantic measured with SOFAR floats. Journal of Geophysical Research 98, 8371–8387.

Sarmiento, J.L., 1986. Three-dimensional ocean models for predicting the distribution of CO_2 between the ocean and atmosphere in the changing carbon cycle: a global analysis, J.R. Trabalka, D.E. Reichle, Ed, Springer–Verlag, New York, 592 pp., 279–294.

Saunders, P.M., 1994. The flux of overflow water through the Charlie-Gibbs Fracture Zone. Journal of Geophysical Research 99, 12,343–12,355.

Schlitzer, R., 1987. Renewal rates of east Atlantic deep water estimated by inversion of ^{14}C data. Journal of Geophysical Research 92, 2953–2980.

Smethie Jr., W.M., 1993. Tracing the thermohaline circulation in the western North Atlantic using chlorofluorocarbons. Progress in Oceanography 31, 51–99.

Smethie Jr., W.M., Swift, J.H., 1989. The Tritium: Krypton-85 age of Denmark strait overflow water and Gibbs fracture zone water just south of Denmark Strait. Journal of Geophysical Research 94, 8265–8275.

Speer, K.G., McCartney, M.S., 1991. Tracing Lower North Atlantic deep water across the equator. Journal of Geophysical Research 96, 20,443–20,448.

Swift, J.H., Aagaard, K., Malmberg, S.A., 1980. The contribution of the Denmark Strait overflow to the deep North Atlantic. Deep-Sea Research 26, 29–42.

Talley L.D., McCartney, M.S., 1982. Distribution and circulation of Labrador Sea Water. Journal of Physical Oceanography 12, 1189–1205.

Tsuchiya, M., Talley, L.D., McCartney, M.S., 1994. Water-mass distributions in the western South Atlantic; a section from South Georgia Island (54S) northward across the equator. Journal of Marine Research 52, 55–81.

Wallace, D.W. R., Lazier, J.R.N., 1988. Anthropogenic chlorofluoromethanes in newly formed Labrador Sea water. Nature 332, 61–63.

Wallace, D.W.R., Beining, P., Putzka, A., 1994. Carbon tetrachloride and chlorofluorocarbons in the South Atlantic Ocean, 19°S. Journal of Geophysical Research 99, 7803–7819.

Warner, M.J., Weiss, R.F., 1985. Solubilities of chlorofluorocarbons 11 and 12 in water and seawater. Deep-Sea Research 32, 1485–1497.

Warren, B.A., Speer, K.G., 1991. Deep circulation in the eastern South Atlantic Ocean. Deep-Sea Research 38(Suppl. 1), S281–S322.

Weiss, R.F., Bullister, J.L., Gammon, R.H., Warner, W.J., 1985. Atmospheric chlorofluoromethanes in the deep equatorial Atlantic. Nature 314, 608–610.

Wüst, G., 1935. Schichtung und Zirckulation des Atlantischen Ozeans, Die Stratosphare. Wissenschaftliche Ergebnisse der Deutschen Atlantisehen Expedition auf dem Forschungsund Vermessungsschiff 'Meteor' 1925–1927, 6, (1), 180, (W.J. Emery, (Ed.), 1978. The Stratosphere of the Atlantic Ocean, Amerind, New Delhi, 112 pp.).